ARMOUR RESEARCH FOUNDATION
of
Illinois Institute of Technology
Technology Center
Chicago 16 Illinois

AD-676331

REVISION OF STANDARDS FOR

MEASUREMENTS OF SHIELDING EFFECTIVENESS OF ENCLOSURES

Fourth Quarterly Progress Report
1 April 1959 - 30 June 1959
Contract No. NObsr - 72824
ARF Project No. E108

For:
Bureau of Ships
Department of the Navy
Washington 25, D. C.

Copy No. _____

ARF Proj. E108
Quar. Rpt. No. 4

REVISION OF STANDARDS FOR
MEASUREMENTS OF SHIELDING EFFECTIVENESS OF ENCLOSURES

ABSTRACT

This report covers the work performed during the fourth quarter of a research program which began on 18 June 1958 and has been extended to 30 September 1959. The program consists of theoretical and experimental investigations leading to an improved standard for testing shielded enclosures in the frequency range of 14 kilocycles to 10,000 megacycles. The improved standard is being formulated in terms of tests at 15 kilocycles, at the lowest natural resonant frequency of the enclosure, and near nine kilomegacycles.

A new method for evaluating shielded enclosures using low-impedance, low-frequency fields is under investigation. This method involves the use of two large rectangular transmitting loops which surround and "immerse" the enclosure in an essentially magnetic field. An average value of the field penetrating the enclosure is obtained using a small pick-up loop in the center of the shielded enclosure. In addition, a small loop probe is used to explore the local field in the neighborhood of wall and door joints.

This new method requires only one measurement for the calculation of shielding effectiveness at low frequencies, since the voltage induced in the pick-up loop without the enclosure may be obtained analytically from the formula given in the report.

Tests to measure the variation of shielding effectiveness with frequency were performed on a sheet of copper, 2.5 mils thick, and on the copper screening material of one shielded enclosure manufacturer. Results of the tests indicate that the variation of shielding effectiveness at low frequencies is almost identical for the selected materials. However, at higher frequencies the sheet copper

ARMOUR RESEARCH FOUNDATION OF ILLINOIS INSTITUTE OF TECHNOLOGY

ARF Proj. E108
Quar. Rpt. No. 4

provides a shielding effectiveness increasing with frequency while the screening material provides a shielding effectiveness decreasing with frequency.

The surface resistances of sheet copper and copper screening material were experimentally measured and the reflection losses at low frequencies were calculated. The values thus found agree with theoretical results already published. These data, plus those obtained experimentally with the coaxial testing device, provide an experimental graph of the shielding effectiveness of copper screening material to plane waves from dc to 400 mc.

A shielded enclosure is a rectangular cavity capable of exhibiting resonances which can produce a high field intensity in the interior of the enclosure due to outside sources, even though the field at the surface of the inner walls is small. Measurements of the resonant frequencies of the parallelepiped enclosure agree well with predicted values. Measurements of the shielding effectiveness of the enclosure at these mid-frequencies are obtained by using a half-wave dipole as the transmitting antenna outside the enclosure and an electrically short (of the order of $\lambda/8$) dipole as the receiving antenna inside. The degradation to shielding effectiveness introduced at these resonant frequencies is about 25 to 30 db.

A coaxial device is utilized for evaluating the shielding effectiveness of materials to plane waves. Plane waves traveling along the coaxial device are incident upon the test lamina and the transmitted portion of these waves can be measured to obtain the shielding effectiveness of materials to plane waves. Experimental results are given for sheet copper, aluminum, stainless and magnetic steels, and high-μ metal on one hand and copper screening on the other. The shielding effectiveness of the former group of materials increases with frequency, whereas that of the copper screening decreases. The coaxial device is also employed to determine the electrical parameters of shielding materials.

TABLE OF CONTENTS

TABLE OF CONTENTS (Cont'd)

ERRATA

LIST OF FIGURES

REVISION OF STANDARDS FOR

MEASUREMENTS OF SHIELDING EFFECTIVENESS OF ENCLOSURES

I. PURPOSE

The purpose of this research is to develop improved techniques for
measuring the effectiveness of shielded enclosures in the frequency range of
14 kilocycles to 10,000 megacycles per second, and to provide recommendations
for standard methods of evaluating such enclosures.

II. GENERAL FACTUAL DATA

A. Identification of Personnel

Name	Title	Man-Hours to End of 3rd Quarter	Man-Hours Total
R. B. Schulz	Research Engineer-Project Engineer	431	515
L. C. Peach	Research Engineer	803	835
D. P. Kanellakos	Assistant Engineer	484	956
L. J. Greenstein	Technical Assistant	136	136
Additional Engineering Services		41	45

B. References

(1) "Electromagnetic Fields", Vol. 1, E. Weber, John Wiley and Sons, Inc.,
New York, 1950.

(2) "Revision of Standards for Attenuation Measurements of Shielded Enclosures",
by L. C. Peach, Third Quarterly Progress Report, Contract No. NObsr-72824,
April 1959.

(3) "Communication Networks", Vol. II, by Ernst A. Guillemin, John Wiley and
Sons, Inc., 1935.

(4) "Antennas", by John D. Kraus, McGraw-Hill Book Co., Inc., New York, 1950.

(5) "Theory, Design and Engineering Evaluation of Radio-Frequency Shielded Rooms",
by C. S. Vasaka, Report No. NADC-EL-5412°, U.S. Naval Air Development Center,
Johnsville, Pennsylvania, 1956.

(6) "Microwave Electronics", by J. C. Slater, D. Van Nostrand Company, Inc.,
New York, 1950.

ARMOUR RESEARCH FOUNDATION OF ILLINOIS INSTITUTE OF TECHNOLOGY

C. <u>Steering Committee Meetings</u>

(1) **Date:** April 16, 1959

    Place: Navy Department, Washington, D. C.

    Personnel Attending:

        Mr. L. W. Thomas, Bureau of Ships

        Mr. A. P. Massey, Bureau of Ships

        Mr. R. B. Schulz, Armour Research Foundation

(2) **Date:** June 15, 1959

    Place: New York

    Personnel Attending:

        Mr. A. P. Massey, Bureau of Ships

        Mr. R. B. Schulz, Armour Research Foundation

        During these steering committee meetings, Mr. R. B. Schulz reviewed the status of the project with Messrs. L. W. Thomas and A. P. Massey and presented plans for the future work on the project.

III. <u>DETAILED FACTUAL DATA</u>

A. <u>Introduction</u>

        The purpose of this program of research is to provide a specification for testing shielded enclosures which will furnish a maximum amount of information regarding the performance of the enclosure, without requiring an undue amount of equipment or effort.

        Theoretical and experimental results at the present time indicate that tests should be performed in three frequency ranges, at 15 kilocycles, at the lowest natural resonant frequency of the enclosure, and near 9 kilomegacycles. The reasons for selecting these frequency ranges will be given in detail in subsequent sections of this report. Briefly, at low frequencies, shielding

against low-impedance fields is much more difficult than other types of fields and, consequently, a test using such fields is believed to be necessary. At mid-frequencies, enclosures exhibit resonance phenomena which significantly affect the performance of the enclosure; a test in this frequency range is therefore suggested. At the very high frequencies, shielded enclosures exhibit behavior not predictable from their performance at lower frequencies and, consequently, a test at these frequencies is advisable. A discussion of the tests performed in the three frequency ranges is contained in Section III-B, -C, and -D respectively.

The performance of a shielded enclosure is largely determined by both the construction of the room and the wall materials. A coaxial device for testing shielded-enclosure materials was discussed in the two previous quarterly progress reports. A more complete discussion of the device is given in Section III-E. The primary problems involved in the development of the device have been the need for equalization of contact resistance between the coaxial holder and the test sample and the employment of very thin samples so that adequate outputs could be obtained. At the present time, the upper frequency limit is about 5 to 8 mc for solid sheets of shielding materials of few mils thickness and about 400 mc for copper screening. The frequency limits differ widely because the shielding effectiveness of the first group goes up with frequency whereas, for the second, the effectiveness decreases. The coaxial device can also be employed to determine the electrical characteristics of materials.

B. Low-Frequency Tests

1. Introduction

Since the presence of low impedance fields at low-frequencies is quite common and these fields are the most difficult to shield against, the shielding

- 3 -

effectiveness of an enclosure should be measured against low-impedance magnetic fields. These low-impedance fields can most easily be produced by current loops whose dimensions are small compared to the wavelength.

2. Low-Impedance Fields

A new method for producing low-impedance magnetic fields for testing the shielded enclosure utilizes two large, square loops completely surrounding the enclosure. The two loops are located near the ceiling and floor of the enclosure, respectively. They are used instead of only one placed in the middle of the enclosure as previously reported, for two reasons: (1) the two loops will not hinder opening and closing of the enclosure door and (2) the two loops will provide a stronger and more uniform magnetic field. The loop-to-enclosure separation is approximately two inches. This separation is a compromise between the effect of capacitance to the room, when the loops are closer to the shield of the enclosure, and the magnitude of shielding currents induced in the walls of the enclosure when the loops are far away from these walls. When a moderate current flows in the turns of the loops, it produces a sufficiently strong magnetic field which completely surrounds all sides of the shielded enclosure. This arrangement allows measurements of the overall performance of the shielded enclosure to be made with simplicity.

3. Measurement of Shielding Effectiveness

Refer to Figure 1. The two loops L.T. and L.B. were placed in parallel horizontal planes equally near the roof and floor of the enclosure, respectively, so that they did not hinder the opening and closing of the enclosure entrance E. To reduce capacitive effects to a minimum but yet provide strong enough fields for detection, and also to provide supports for the loops, hooks H were placed in the eight corners of the enclosure. These were ordinary rubber suction cups

ARF Proj. E108
Quar. Rpt. No. 4
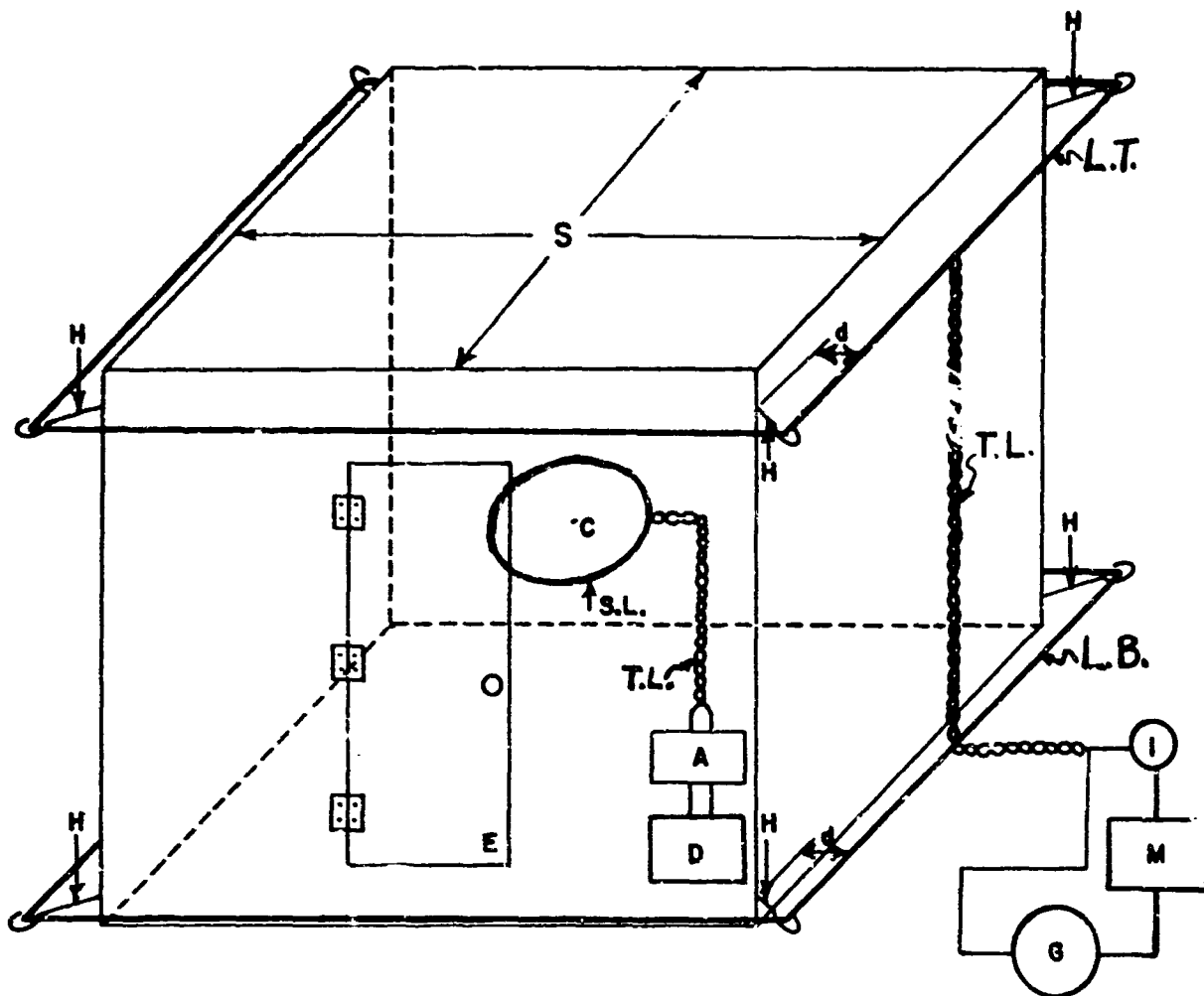
Frequency of test: 15×10^3 cps

C   = Center of shielded enclosure   E   = Enclosure entrance
S   = Outer shielding layer   H   = Hooks of sufficient length to allow d
d   = 2 inches   T.L.= Twisted leads
L.T. = Top loop   (Each 10 turns of No. 18 insulated wire horizontally oriented and)
L.B. = Bottom loop (engulfing the entire closure. (Transmitting antenna.)   )
S.L. = Circular loop. Antenna AT-205/URM-6 used in conjunction with Radio Interference
        Set AN/URM-6 or 10-turn, 12-inch diameter of No. 12 AWG copper enameled insulated
        wire. Placed in the center of the room midway between L.T. and L.B.
        (Receiving antenna)
G   = Low impedance signal source to obtain adequate output at frequency of test
I   = Audio frequency A.C. ammeter good at 15 kc. (The voltage across a 1-ohm non-
        inductive resistor may be measured to find I.)
M   = Impedance matching transformer, if necessary
D   = Radio Interference Set AN/URM-6 or high input impedance A.C. voltmeter
A   = Low noise, narrow bandpass amplifier, if necessary.

FIG. 1 SHIELDING EFFECTIVENESS MEASUREMENT - LOW IMPEDANCE FIELDS

RUBBER SUCTION CUP
Available at any
Hardware Store

A

METAL HOOK
No. 12 AWG Copper Wire
Bent to Shape

8-32 Machine
Screw
&
Nut
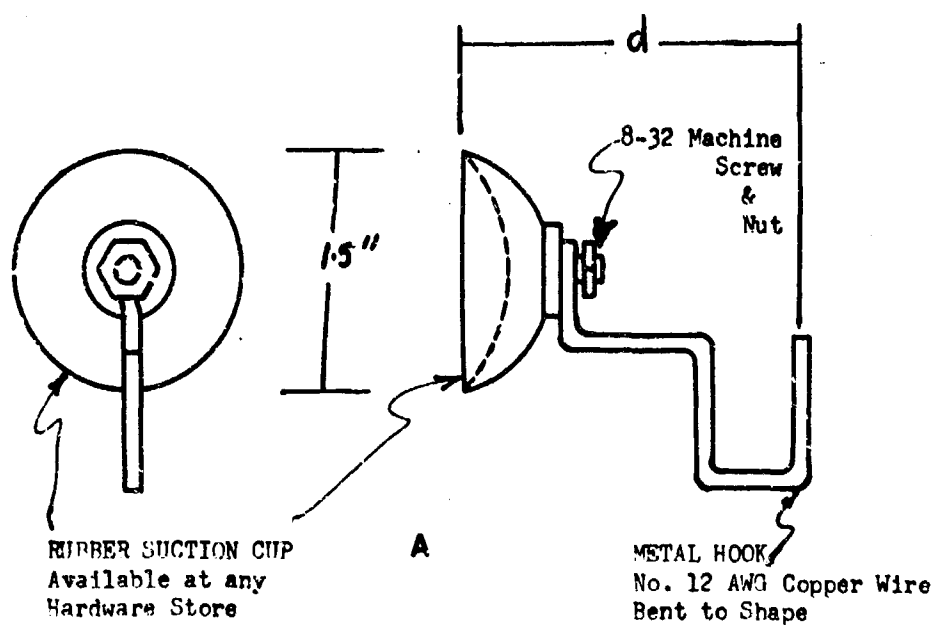
d = approximately two inches

FIG. 1A   RUBBER SUCTION CUP WITH METAL HOOK

with hooks like those in Figure I A. Protrusion of the hooks was such as to allow a distance of approximately 2 inches between the loops and the enclosure outer shielding layer S.

Each loop consisted of 10 turns of No. 18 stranded, tinned, insulated copper wire; the turns were spaced as closely as possible. The two loops were connected in series aiding with twisted leads T.L. which were also connected to an audio signal generator or power oscillator G. An impedance matching transformer M was used to match the output impedance of the generator to that of the external loops. The impedance of the latter was measured with an a.c. impedance bridge at the frequency of test and in its final test position. Inside the enclosure at its center was placed a pick-up loop S.L. similar to antenna AT-205/URM-6 or alternatively, a 10 turn, 12-inch enamel-insulated wire pick-up loop. The plane of the pick-up loop was parallel to the planes containing L.T. and L.B. The output of the signal generator G was adjusted until a sufficient current I was flowing in the turns of the big outside loops which induced a measurable voltage in the small inside loop. The voltage induced in the small loop at the center of the room, while the large loops were excited, was measured with the calibrated Radio Test Set AN/URM-6 or, alternatively, with a high impedance voltmeter. The high impedance voltmeter limits the current flowing in the small inside loop to a minimum (this current should be essentially zero since, if it were not zero, it would create an additional magnetic field which would tend to cancel those produced by the large loops and thus introduce an error in the measurement). A low noise, narrow band amplifier A with a high input impedance was used when the output signal of the small loop was insufficient to give a reading at the detector D. The voltage induced in the pick-up loop without the presence of the shielded enclosure under the same conditions described above

was calculated theoretically from

$$(1) \qquad V_2 = 2\pi f N_1 A B_z \quad \text{volts}$$

where

$$(1A) \qquad B_z = \frac{2\mu_0 N I ab}{\pi} \; \frac{1}{\sqrt{a^2 + b^2 + d^2}} \left\{ \frac{1}{a^2 + d^2} + \frac{1}{b^2 + d^2} \right\}$$

f = frequency of test (15×10^3 cps)

N_1 = number of turns of small pick-up loop

A = area of small pick-up loop in square meters

μ_0 = $4\pi \times 10^{-7}$ henry/meter, permeability of free space

N = Number of turns in each of big loops

I = current in amperes

$2a$ = x-dimension of big loop in meters
$2b = y - $ '' $\quad$ '' $\quad$ '' $\quad$ '' $\quad$ ''
$2d$ = separation of the two big loops center-to-center in meters.

The shielding effectiveness is defined as

$$(2) \qquad \text{Shielding Effectiveness (db)} = 20 \log \frac{H_1}{H_2}$$

where

H_1 = the magnetic field intensity without the enclosure

H_2 = the magnetic field intensity within the enclosure

Since the voltages thus calculated and measured are proportional to the magnetic field intensities H_1 and H_2, respectively, the shielding effectiveness is calculated from equation

$$(3) \qquad \text{Shielding Effectiveness (db)} = 20 \log \frac{V_1}{V_2}$$

- 8 -

where

V_1 = the theoretically determined open circuited voltage induced in the pick-up loop without the enclosure in volts

V_2 = the open circuited voltage induced in the pick-up loop within the enclosure in volts.

A test was made to insure that no case leakage existed at the detector. The detector showed no indication whatever above the inherent background when the generator G was disconnected. While the loops were in the positions shown in Figure 1, a small loop probe was used to search for leaks and other imperfections that were present. The small probe was a multiturn unit AN-207/URM-6 used in conjunction with an AN/URM-6 Radio Test Set. When the small loop probe was carried in a horizontal plane around the enclosure walls, a variation of the pick-up voltage resembled the illustration given in Figure 2. The joints were tightened until the peaks of the leaky joints, at all joints, were reduced to a minimum. Other places which appeared leaky were corrected.

Only after all the joints were well tightened and all other defects had been corrected, the shielding effectiveness low frequency test, as described above, was performed. Typical values of shielding effectiveness ranged around 60 db for a cell-type screened enclosure of old manufacture.

It is proposed that this test procedure be included in the revised test standards for measuring shielding effectiveness of shielded enclosures.

4. Theoretical Derivation of Equation (1A)

The theoretically expected value of the voltage induced in a small single-turn circular loop when placed along the axis and parallel with a large rectangular loop of sides 2a or 2b meters in the xy-plane, as shown in Figure 3, will be derived for a current of I amperes flowing in the rectangular loop, whose conductor cross section is considered small compared with 2a and 2b.

ARMOUR RESEARCH FOUNDATION OF ILLINOIS INSTITUTE OF TECHNOLOGY

- 9 -
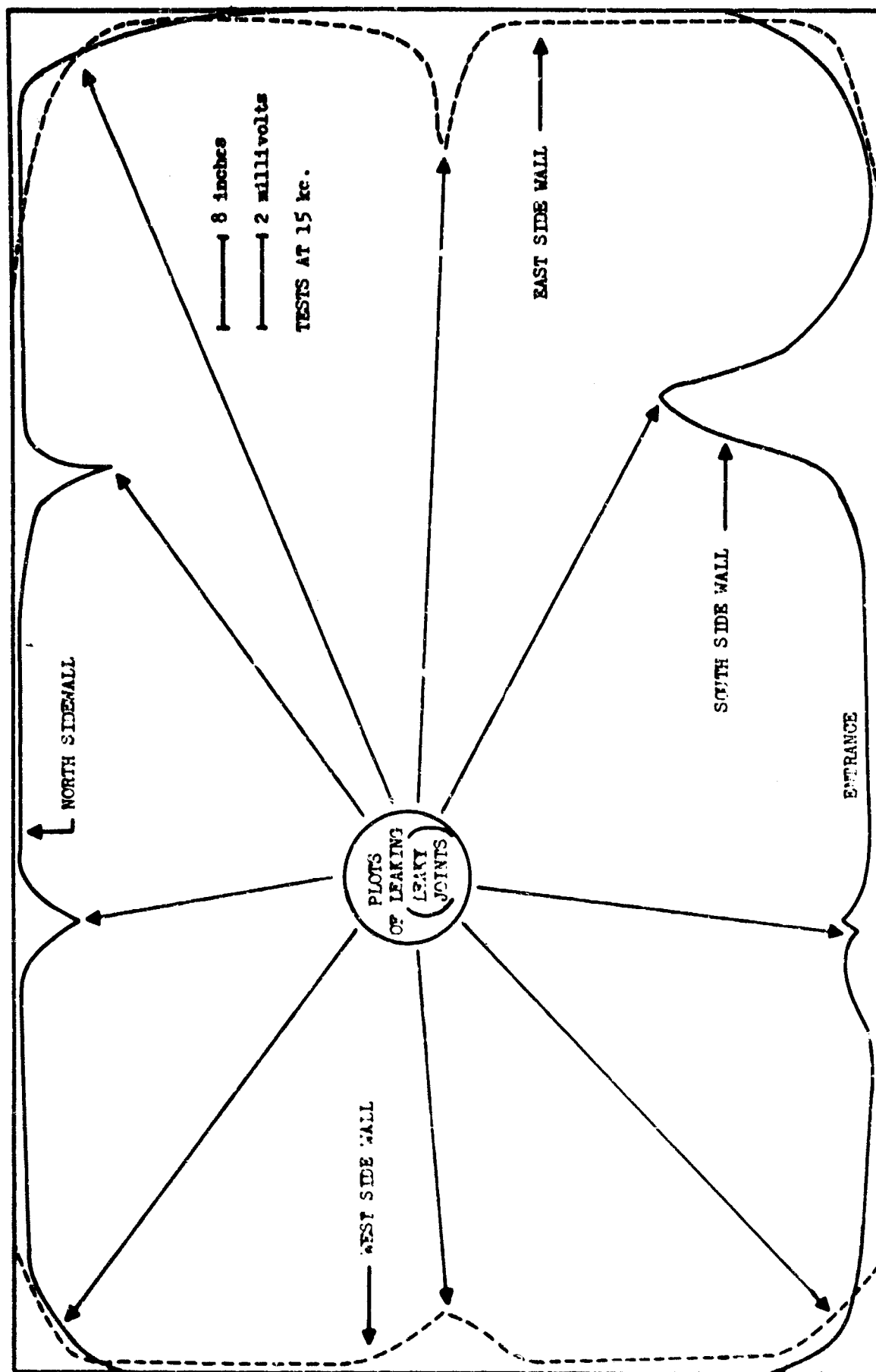
FIG. 2 PLAN VIEW OF SHIELDED ENCLOSURE SHOWING LEAKY JOINTS

EAST SIDE WALL

SOUTH SIDE WALL

ENTRANCE

NORTH SIDEWALL

WEST SIDE WALL

PLOTS OF LEAKING (LEAKY JOINTS)

| 8 inches
| 2 millivolts

TESTS AT 15 kc.

- 10 -
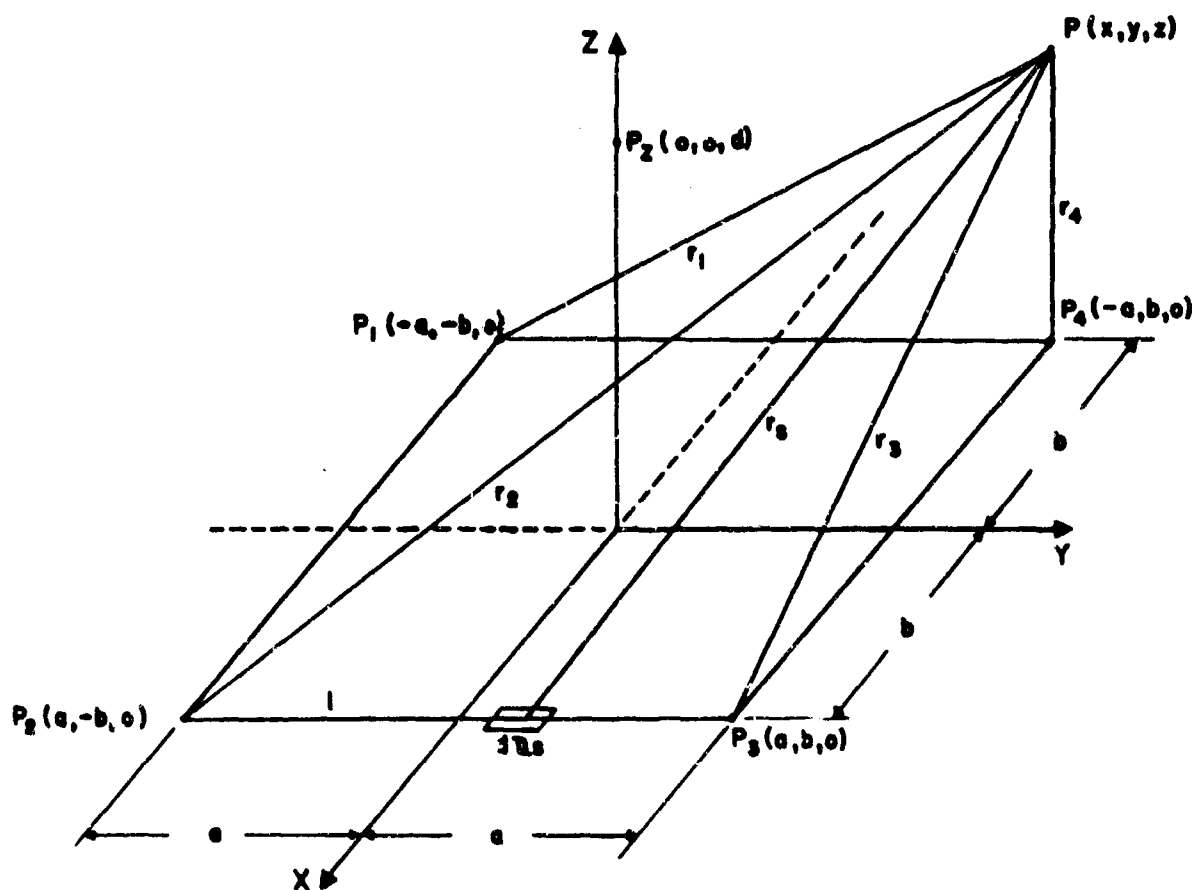
$$r_1^2 = (x+a)^2 + (y+b)^2 + z^2$$

$$r_2^2 = (x-a)^2 + (y+b)^2 + z^2$$

$$r_3^2 = (x-a)^2 + (y-b)^2 + z^2$$

$$r_4^2 = (x+a)^2 + (y-b)^2 + z^2$$

FIG. 3 FIELD DUE TO A RECTANGULAR LOOP

The incremental vector potential at a distance r_s from an element of a conductor of length $d\ell_s$ carrying a current I amperes is given by

$$(4) \qquad d\mathbf{A} = \frac{\mu I}{4\pi} \frac{d\ell_s}{r_s}$$

and the total vector potential $\mathbf{A}$ may be obtained by integrating around the closed loop

$$(5) \qquad \mathbf{A} = \frac{\mu I}{4\pi} \oint \frac{d\ell_s}{r_s} \, .$$

For the rectangular loop, $\mathbf{A}$ has two components A_x and A_y given by[1]

$$(6) \qquad A_x = \frac{\mu I}{4\pi} \, \ell n \, \frac{(r_1 + a + x)}{(r_2 - a + x)} \frac{(r_3 - a + x)}{(r_4 + a + x)}$$

and

$$(7) \qquad A_y = \frac{\mu I}{4\pi} \, \ell n \, \frac{(r_2 + b + y)}{(r_3 - b + y)} \frac{(r_4 - b + y)}{(r_1 + b + y)} \, ,$$

where r_1, r_2, r_3, r_4 are the distances from the point P to the individual vertices of the rectangular loop, respectively. Since the small loop is placed with its center along the z-axis and is parallel to the large loop, B_x and B_y will not contribute to the induced voltage in the loop. The flux density in the plane of the loop is given by

$$(8) \qquad B_z = \frac{\partial}{\partial x} A_y - \frac{\partial}{\partial y} A_x \, .$$

Eq. (8) is completely general and is derived from

$$(9) \qquad \mathbf{B} = \nabla \times \mathbf{A} \, ,$$

where

[1] Reference 1, pp. 132-134.

(10) $\qquad \nabla = 1_x \dfrac{\partial}{\partial x} + 1_y \dfrac{\partial}{\partial y} + 1_z \dfrac{\partial}{\partial z}$.

For a point $P(o, o, z)$,

(11) $\qquad r_1 = r_2 = r_3 = r_4 = \sqrt{a^2 + b^2 + z^2}$

and both A_x and A_y are zero.

Since

(12) $\qquad \dfrac{d}{dx} \ln u(x, y, z) = \dfrac{1}{u} \dfrac{du}{dx}$,

the partial derivatives in Equation (8) may be evaluated more easily if one lets

(13a) $\qquad u(x, y, z) = \dfrac{(r_2 + b + y)}{(r_3 - b + y)} \dfrac{(r_4 - b + y)}{(r_1 + b + y)} = \dfrac{(N_1)(N_2)}{(D_1)(D_2)}$,

and

(13b) $\qquad v(x, y, z) = \dfrac{(r_1 + a + x)}{(r_2 - a + x)} \dfrac{(r_3 - a + x)}{(r_4 + a + x)} = \dfrac{(N_1')(N_2')}{(D_1')(D_2')}$.

Thus,

(14) $\qquad \dfrac{\partial}{\partial x} A_y = \dfrac{\mu I}{4\pi} \dfrac{\partial}{\partial x} \ln u = \dfrac{\mu I}{4\pi} \dfrac{1}{u} \dfrac{d}{dx} \dfrac{(r_2 + b + y)}{(r_3 - b + y)} \dfrac{(r_4 - b + y)}{(r_1 + b + y)}$.

(15) $\qquad \dfrac{\partial}{\partial x} A_y = \dfrac{k}{u} \dfrac{D_1 D_2 (N_1 \frac{dr_4}{dx} + N_2 \frac{dr_2}{dx}) - N_1 N_2 (D_1 \frac{dr_1}{dx} + D_2 \frac{dr_3}{dx})}{(D_1 D_2)^2}$,

where

(16) $\qquad k = \dfrac{\mu I}{4\pi}$.

Thus,

(17) $\qquad \dfrac{\partial}{\partial x} A_y = \dfrac{k}{u} \dfrac{1}{D_1 D_2} \left\{ N_1 \dfrac{x + a}{r_4} + N_2 \dfrac{x - a}{r_2} - u \left[D_1 \dfrac{x + a}{r_1} + D_2 \dfrac{x - a}{r_3} \right] \right\}$

We want to evaluate (17) at the point P_z (o, o, d). Thus, from (11) and (13a),

(18) $\quad u(o, o, d) = 1$.

Therefore, at $P(c, o, d)$,

(19) $\quad \dfrac{\partial A_y}{\partial x} = \dfrac{k}{(r-b)(r+b)} \left\{ \left[\dfrac{r+b}{r} (x+a) + \dfrac{(r-b)}{r} (x-a) \right] - \left[\dfrac{r-b}{r} (x+a) + \dfrac{(r+b)(x-a)}{r} \right] \right\}$

(20) $\quad \dfrac{\partial A_y}{\partial x} = \dfrac{k}{r^2 - b^2} \left\{ \dfrac{r+b}{r} \left[(x+a) - (x-a) \right] + \dfrac{r-b}{r} \left[(x-a) - (x-a) \right] \right\}$

(21) $\quad \dfrac{\partial A_y}{\partial x} = \dfrac{k}{r^2 - b^2} \left[\dfrac{r+b}{r} 2a + \dfrac{r-b}{r} (-2a) \right]$,

(22) $\quad \dfrac{\partial A_y}{\partial x} = \dfrac{k}{r^2 - b^2} \left(\dfrac{2ab}{r} + \dfrac{2ab}{r} \right)$,

(23) $\quad \dfrac{\partial A_y}{\partial x} = \dfrac{k \, 4ab}{(r^2 - b^2) \, r}$.

Finally, Equations (16) and (11) are used to obtain

(24) $\quad \dfrac{\partial A_y}{\partial x} = \dfrac{\mu I ab}{\pi (a^2 + d^2)} \dfrac{1}{\sqrt{a^2 + b^2 + d^2}}$.

Similarly,

(25) $\quad \dfrac{\partial A_x}{\partial y} = k \dfrac{\partial}{\partial y} \ln V (x, v, z)$

and

(26) $\quad \dfrac{\partial A_x}{\partial y} = - \dfrac{\mu I \, ab}{\pi (b^2 + d^2)} \dfrac{1}{\sqrt{a^2 + b^2 + d^2}}$.

Thus,

(27)
$$B_z\Big|_{o,\,o,\,d} = \frac{\mu I\,ab}{\pi\sqrt{a^2+b^2+d^2}}\left(\frac{1}{a^2+d^2}+\frac{1}{b^2+d^2}\right)\frac{webers}{meter^2}\,.$$

Note that equation (27) reduces to Equation (5) of reference 2, page 8, for the case $d = 0$; namely,

(28)
$$B_z\Big|_{o,\,o,\,o} = \frac{\mu I}{\pi}\frac{\sqrt{a^2+b^2}}{ab}\frac{webers}{meter^2}\,.$$

In the case of the contribution of two loops (small loop placed midway between two parallel N turn loops carrying I amperes in their conductors),

(29)
$$B_z = \frac{2N\,\mu I\,ab}{\pi}\frac{1}{\sqrt{a^2+b^2+d^2}}\left(\frac{1}{a^2+d^2}+\frac{1}{b^2+d^2}\right)\frac{webers}{meter^2}\,.$$

The voltage induced in a N_1-turn loop of area A at the point P (o, o, d) is therefore

(30)
$$V = 2\pi f N_1\,\Delta B_z \quad volts$$

or

(31)
$$V = 4NN_1\mu f I A\frac{ab}{\sqrt{a^2+b^2+d^2}}\left(\frac{1}{a^2+d^2}+\frac{1}{b^2+d^2}\right)\quad volts$$

Equation (27) is exactly Equation (1A) mentioned above and Equation (31) is similar to Equation (1).

5. Reciprocity of Shielding Effectiveness Measurements by the Two-Loop Method

The basic method of measuring shielding effectiveness of enclosures at low frequencies involves the use of two loops of unequal size. Placing the larger loop around the enclosure and the smaller one inside the enclosure, one can (a) detect the voltage induced in the small loop by the magnetic field created by the large loop; or (b) excite the small loop inside the enclosure and detect the voltage induced in the large loop outside the enclosure.

In both cases, the coupling between the coaxial loops is also calculated (or measured) in the absence of the enclosure. If in the presence and absence of the shielded enclosure the induced voltages measured are designated by V_3 and V_3' for case (a) and V_1 and V_1' for case (b), respectively, the shielding effectiveness is defined by

$$(32) \qquad S.E_{(a)} = 20 \log \left| \frac{V_3'}{V_3} \right| \quad \text{decibels}$$

or

$$(33) \qquad S.E_{(b)} = 20 \log \left| \frac{V_1'}{V_1} \right| \quad \text{decibels.}$$

Reciprocity shows that, if the open-circuited voltages are measured by a high impedance voltmeter, the two insertion loss values obtained in both methods are equivalent; that is,

$$(34) \qquad S.E_{(a)} = S.E_{(b)}.$$

To show the validity of Equation (34) analytically, consider an over-simplified, but adequate for the purposes of this analysis, circuit diagram of the measurement setup shown in Figure 4. In this figure, the shielded enclosure is represented by a short-circuited turn. A voltage of V_1 volts rms impressed
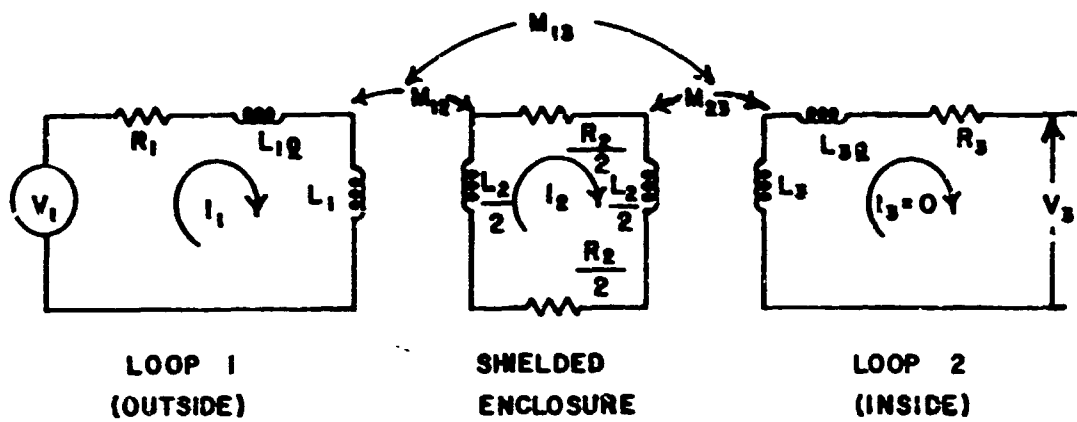
MEASUREMENT (a)
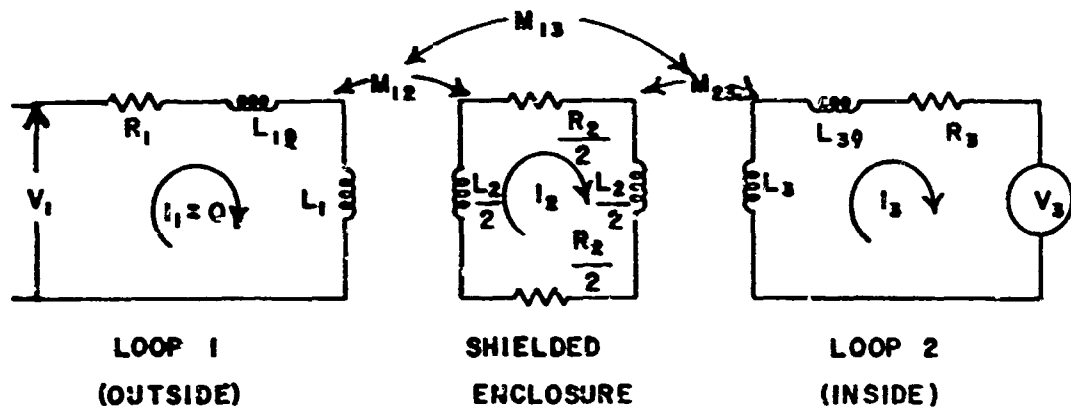
MEASUREMENT (b)

$L_{1\ell}$, $L_{3\ell}$ ARE LEAKAGE INDUCTANCES
L_1 , L_2 , L_3 ARE SELF INDUCTANCES
M_{12} , M_{23} , M_{13} ARE MUTUAL INDUCTANCES

FIG. 4 SIMPLIFIED CIRCUIT DIAGRAM OF THE TWO LOOP METHOD OF MEASURING SHIELDING EFFECTIVENESS OF ENCLOSURES AT LOW FREQUENCIES

by a generator located in the first (transmitting) loop will cause a current of I_1 amperes rms to flow in this loop. This current induces I_2 amperes rms to flow in the enclosure walls. The currents I_1 and I_2 induce a voltage V_3 in the loop inside. No current is allowed to flow in the second (receiving) loop because of the high impedance of the voltmeter used to measure the voltage across this loop.

The voltage equations of the systems are (see Figure 4(a)), since $I_3 = 0$,

$$(35) \qquad -V_3 = j\omega M_{13} I_1 - j\omega M_{23} I_2$$

and

$$(36) \qquad 0 = j\omega M_{12} I_1 + (R_2 + j\omega L_2) I_2 .$$

From Equations (35) and (36),

$$(37) \qquad V_3 = \left(-j\omega M_{13} + \frac{j\omega M_{23} j\omega M_{12}}{R_2 + j\omega L_2} \right) I_1 .$$

Now the middle mesh is removed; this corresponds to removing the shielded enclosure. Mesh No. 1 is again excited until a current of I_1 amperes rms flows in it. The open circuited voltage in Mesh No. 3 is therefore

$$(38) \qquad -V_3' = j\omega M_{13} I_1 .$$

Using Equations (37) and (38) in Equation (32) and simplifying, one gets

$$(39) \qquad S.E_{(a)} = 20 \log \left| \frac{R_2 + j\omega L_2}{R_2 + j\omega (L_2 - \frac{M_{12} M_{23}}{M_{13}})} \right| .$$

By a similar procedure, but now exciting the loop inside and measuring the

open circuited voltages V_1 and V_1' induced in the big loop outside (see Figure 4(b)), it is found that

$$(40) \qquad S.E_{(b)} = 20 \log \left| \frac{R_2 + j\omega L_2}{R_2 + j\omega(L_2 - \frac{M_{12} M_{23}}{M_{13}})} \right|$$

Comparing Equations (39) and (40), one sees that Equation (34) is justified. It is interesting to notice that

$$(41) \qquad \lim_{\omega \to 0} \left| \frac{V_i'}{V_i} \right| \Longrightarrow 1, \qquad i = 1, 2.$$

and Equations (39), (40) and (41) agree with experimental results which show that the shielding effectiveness of the enclosure to low-impedance fields at very low frequencies is zero[1] (log 1 = 0).

A similar analysis of Figures 4(a) and 4(b), but now allowing currents I_3 and I_1 to flow in Mesh No. 3 and Mesh No. 1, respectively, (case of the low impedance voltmeter), shows that the corresponding Equations (39) and (40) are not equal.

Thus, as long as no current is allowed to flow in the pick-up loop, the measurement of shielding effectiveness is bi-lateral. This means that the shielding effectiveness obtained from measurements made by exciting the large loop outside and measuring the open circuit voltage induced in the small loop inside or exciting the small loop inside and measuring the open circuit voltage induced in the large loop outside must be the same. This conclusion was verified experimentally at 15 kc.

---

[1] Reference 2, Figures 4 to 11.

- 19 -

The overall performance of the enclosure is much more effectively checked when the large loop is excited. This method of excitation produces stronger fields near the walls of the enclosure where they are needed to provide stronger currents to check leaky joint and other defects. The small loop is less effective in bathing the entire shielded enclosure with strong enough fields to be detected locally with ease.

Finally, the voltage induced in the small loop inside is measured in the presence of the shielded enclosure while the large loop is excited; this result is compared with the theoretically expected induced voltage in the small loop with the absence of the enclosure. This theoretically-obtained value of induced voltage is the open circuited one. When a current is allowed to flow in the pick-up loop, it will tend to cancel part of the field produced by the large loop. (In the case of Radio Test Set AN/URM-6, the loop pick-up is calibrated in terms of the actual magnetic field so that this is no longer of concern.)

6. Surface Impedance Measurements

Measurements of shielding effectiveness at low frequencies, made with the coaxial testing device[1] on one hand, and with the two loop method[2] on the other, at low frequencies, on copper screening material used by one shielded enclosure manufacturere revealed that it was approximately equal to that offered by a 3-mil-thick copper sheet.

The coaxial device measures the shielding effectiveness of materials to (medium-impedance) plane waves, whereas the two loop method measures the shielding effectiveness to low-impedance magnetic fields. At low frequencies,

---

[1]A discussion of this testing device and its utilization in measuring shielding effectiveness of materials are given in Section III-E of this report

[2]Reference 2, pp. 4 to 14.

ARF Proj. E108
Quar. Rpt. No. 4

the main loss introduced by shielding materials to plane waves is that due to reflection[1]. Since both materials exhibit approximately the same loss at low frequencies, their surface impedances must also be approximately equal. To verify this statement experimentally, the surface impedance of copper sheet 2.5 mils thick and copper screening material, 22 x 22 strands per inch, 15 mils diameter, was measured by the method indicated in Figure 5. The values recorded were 2.24×10^{-4} ohms per square and 2.69×10^{-4} ohms per square for the copper sheet and copper screening material, respectively. The method of measurement used during this test differs from the conventional method[2] in which the electrodes are placed in opposite sides of the square piece whose surface impedance is desired, rather than in adjacent sides. The latter method was used because of the anisotropy of the screening material.

Additional tests were performed to determine the shielding effectiveness of the materials to low-impedance magnetic fields and plane waves at low frequencies. The two-loop method was used to take the data which are plotted in Figure 6. Because of availability, 2.5-mil-thick copper sheet was used for the tests and compared with the shielding of one and two layers of copper screening. Figures 14 and 19, in another section of this report, show the shielding effectiveness of the two materials to plane waves. The shielding effectiveness of the two shielding materials to both low-impedance magnetic fields and plane waves is equivalent only at low frequencies (of the order of a few kc) where it is primarily due to reflection. At higher frequencies, the screen perforations play a more important role and the shielding effectiveness of copper sheet and copper screening are quite different, as shown in Figures 14 and 19, respectively.

---

[1] Reference 5, graph on p. 16
[2] Reference 4, pp. 364-365.
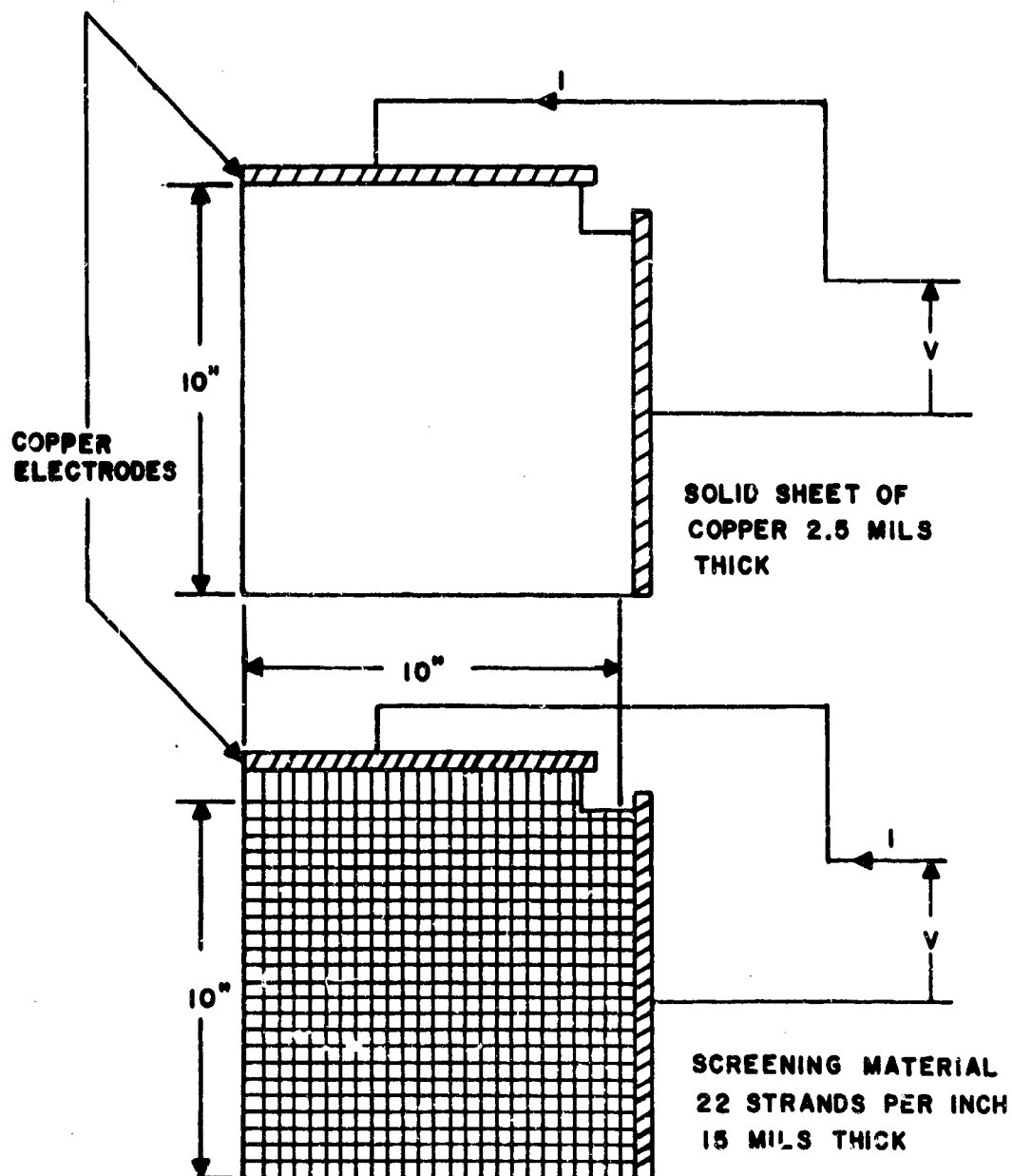
Surface Resistance $R_s = \frac{V}{I}$ (ohms per square)

$R_s = 2.69 \times 10^{-4}$ ohms/square, for copper screening

$R_s = 2.24 \times 10^{-4}$ ohms/square, for copper sheet

FIG. 5 SURFACE RESISTANCE OF SCREENING MATERIALS

COPPER: $R_r = 1.0$
RELATIVE PERMEABILITY $\mu_r = 1.0$
EXPERIMENTALLY OBTAINED
CURVES: SOLID LINES

2.5 mil thick
Copper Sheet

One layer of
Copper Screen,
22 x 22 strands
per inch, 15 mils
diameter

Two layers of
of copper screen,
22 x 22 strands
per inch, 15 mils
Layers one inch
apart.

RATIO OF FLUX LINKAGES, N, db

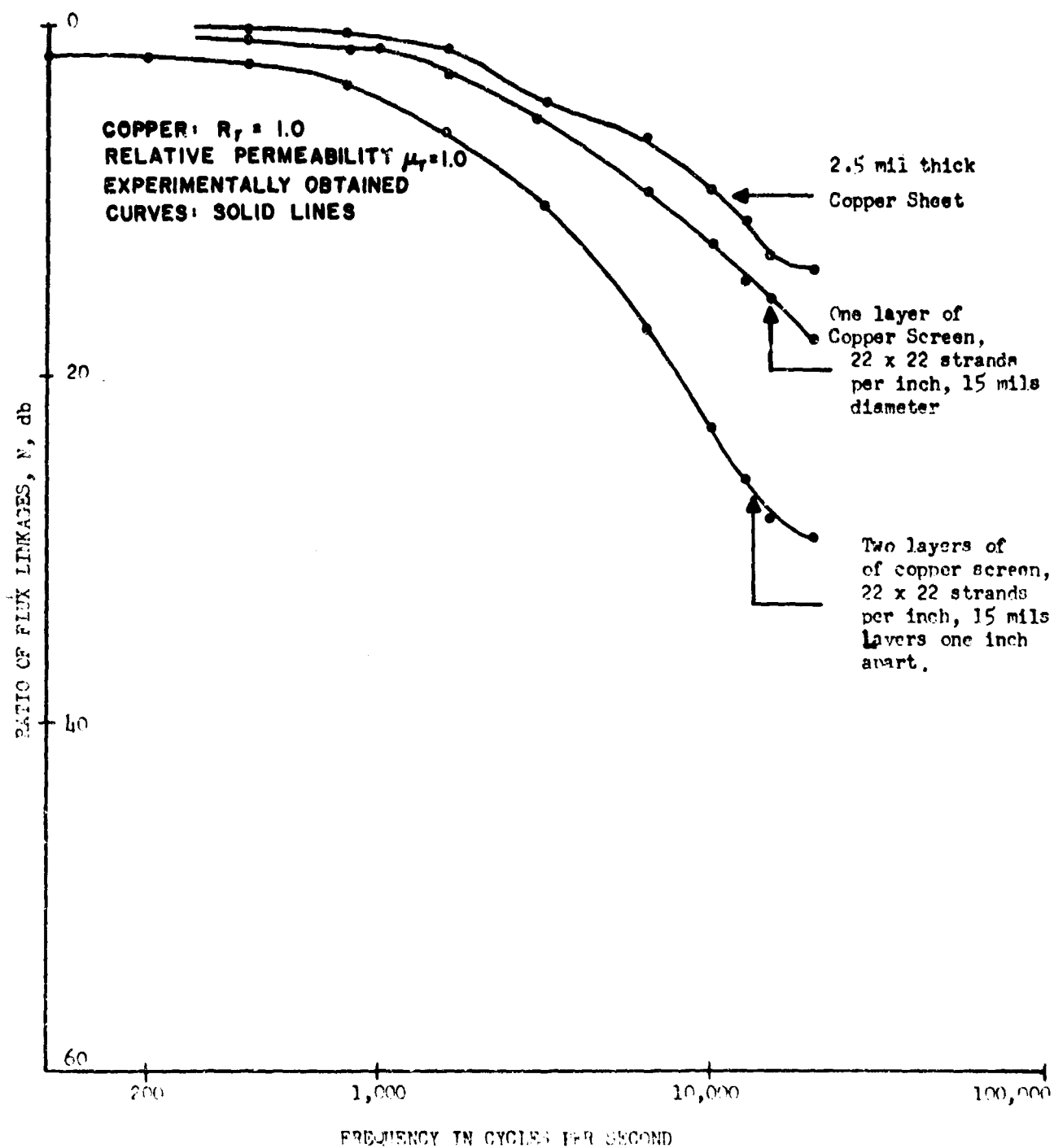FREQUENCY IN CYCLES PER SECOND

FIG. 6 TWO LOOP METHOD OF MEASURING SHIELDING EFFECTIVENESS

- 29 -

The reflection loss in db sustained by a plane wave incident on the above materials is calculated from[1]

$$(42) \qquad \text{R.L. (db)} = 20 \log \frac{(R_s + 377)^2}{4R_s \, 377},$$

with the justifiable assumption of

$$(43) \qquad R_s \ll 377.$$

Calculated reflection loss at d.c. leads to values of 152.5 db and 150.9 db for the copper sheet and screening material, respectively. These values of reflection loss are in agreement with the 150 db (100 cps) theoretical value reported by Vasaka[2].

In section III-E of this report, additional experimental data are given regarding the variation with frequency of shielding effectiveness to plane waves of different screening materials acting as shields.

C. Measurements at Mid-Frequencies

1. Introduction

In the Third Quarterly Progress Report, it was pointed out that the shielding enclosure acts as a resonant cavity at the frequencies at which its sides are equal to $n \frac{\lambda}{2}$, where n is an integer and λ is the wavelength of electromagnetic waves at frequency f. The existing standing waves inside the "cavity" can affect any electrical equipment in an unfavorable manner whenever it is placed at locations where the field intensity is high because of resonance. Some of the resonance frequencies calculated for the shielded enclosure under test were 83.4 mc., 167 mc., 184 mc., 210 mc., etc.[3] Figure 13, p. 32, of

---

[1] Reference 5, pp. 3-5.

[2] Ibid., graph on p. 16

[3] Reference 2, pp. 29-31

ARF Proj. E108
Quar. Rpt. No. 4

Reference 2 shows the distribution of the electric and magnetic fields for the TE_{101} mode and one method of its excitation[1].

2. Experimental Results

a. Introduction

Attempts were made to detect the predicted resonant frequencies of the cell-type, copper screened enclosure of approximate dimensions of 10 feet x 8 feet x 8 feet. The resonances are hard to find because the Q of the cavity is very high. With the calculated resonant frequencies as a guide, measurements were made of the existing fields inside the room. The set-up shown in Figure 7 was used to obtain the curves appearing in Figures 8, 9, and 10. As can be seen from these figures, the degradation to shielding effectiveness introduced at the lowest group of resonant frequencies is about 30 db.

b. Method of Measuring Shielding Effectiveness

The measurement of the shielding effectiveness at the mid-frequencies is accomplished by using the measurement set-up shown in Figure 7. Because of the high attenuation introduced by the shielded enclosure at the mid-frequency region, a high power signal generator was used, specifically a Rollin Power Type Signal Generator, Model 30A. The generator was feeding a half-wave dipole antenna A_2 through a 50-ohm doubly shielded cable (RG/U-9B) C_2; the antenna A_2 produces in the vicinity of the enclosure strong free field waves whose impedance is that of plane waves. Inside the enclosure was placed another dipole antenna A_1 whose length ℓ_1 is much less than a quarter wavelength at the frequency of test. The overall length of the dipole receiving antenna is kept electrically short $(\frac{\lambda}{8} \leq \ell_1 < \frac{\lambda}{4})$ so that its impedance will not change

---

[1] For corrections to this figure, see ERRATA at the end of this report.
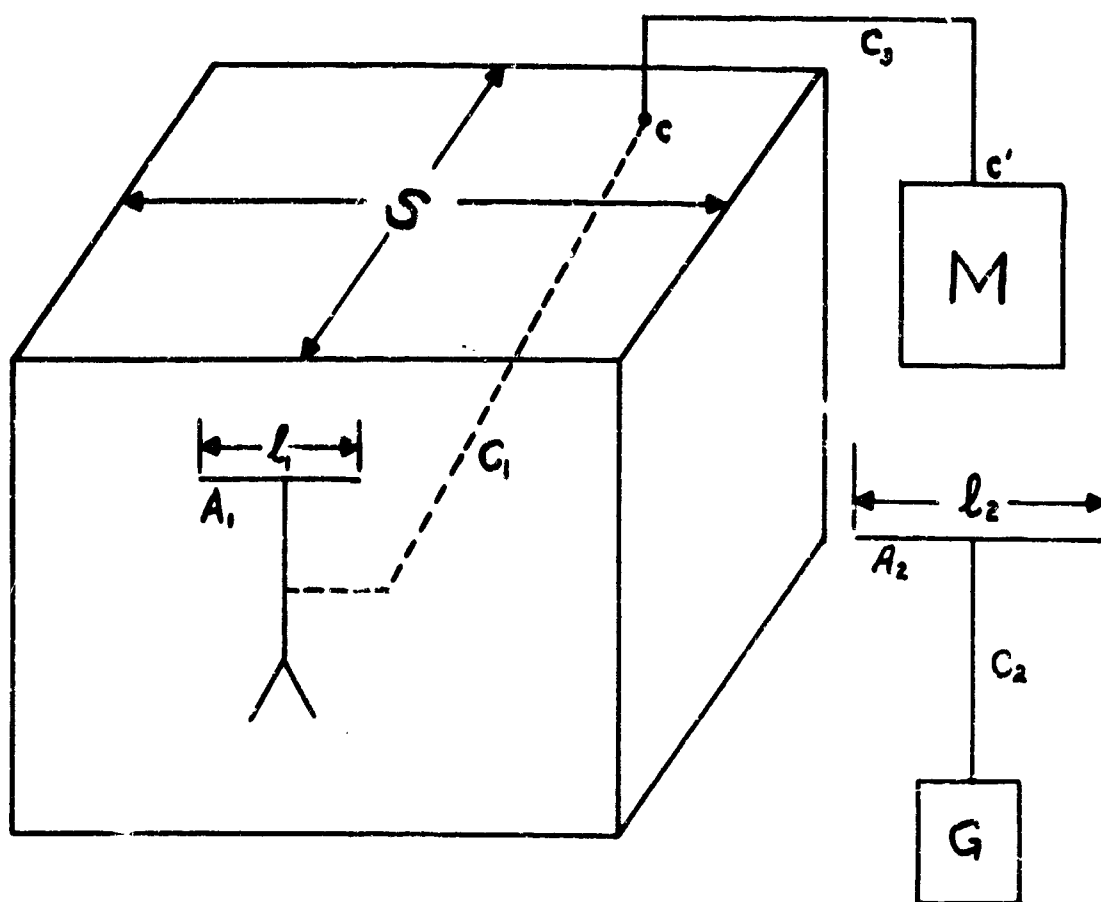
S = Enclosure Shielding Layers

G = High Power Generator suitable to obtain adequate output at the frequency of test: Rollin Power Type Standard Signal Generator Model 31A

A_2 = Transmitting Half-Wave Dipole Antenna. $\ell_2 = \lambda/2$

A_1 = Receiving Short Dipole Antenna. $\ell_1 \leq \lambda/8$

M = Radio Interference Measuring Set AN/URM-47

C_1, C_2, C_3 connecting shielded coaxial cables.

Frequency of test: The lowest natural resonant frequency of the enclosure considered as a cavity. In the case of a rectangular parallelepiped enclosure the frequency is

$$f = 150\sqrt{\frac{1}{a^2} + \frac{1}{b^2}} \quad \text{megacycles}$$

Where a and b are the inside dimensions of the edges which form the larger side wall of the enclosure expressed in meters.

FIG. 7 SHIELDING EFFECTIVENESS MEASUREMENT - MID-FREQUENCIES
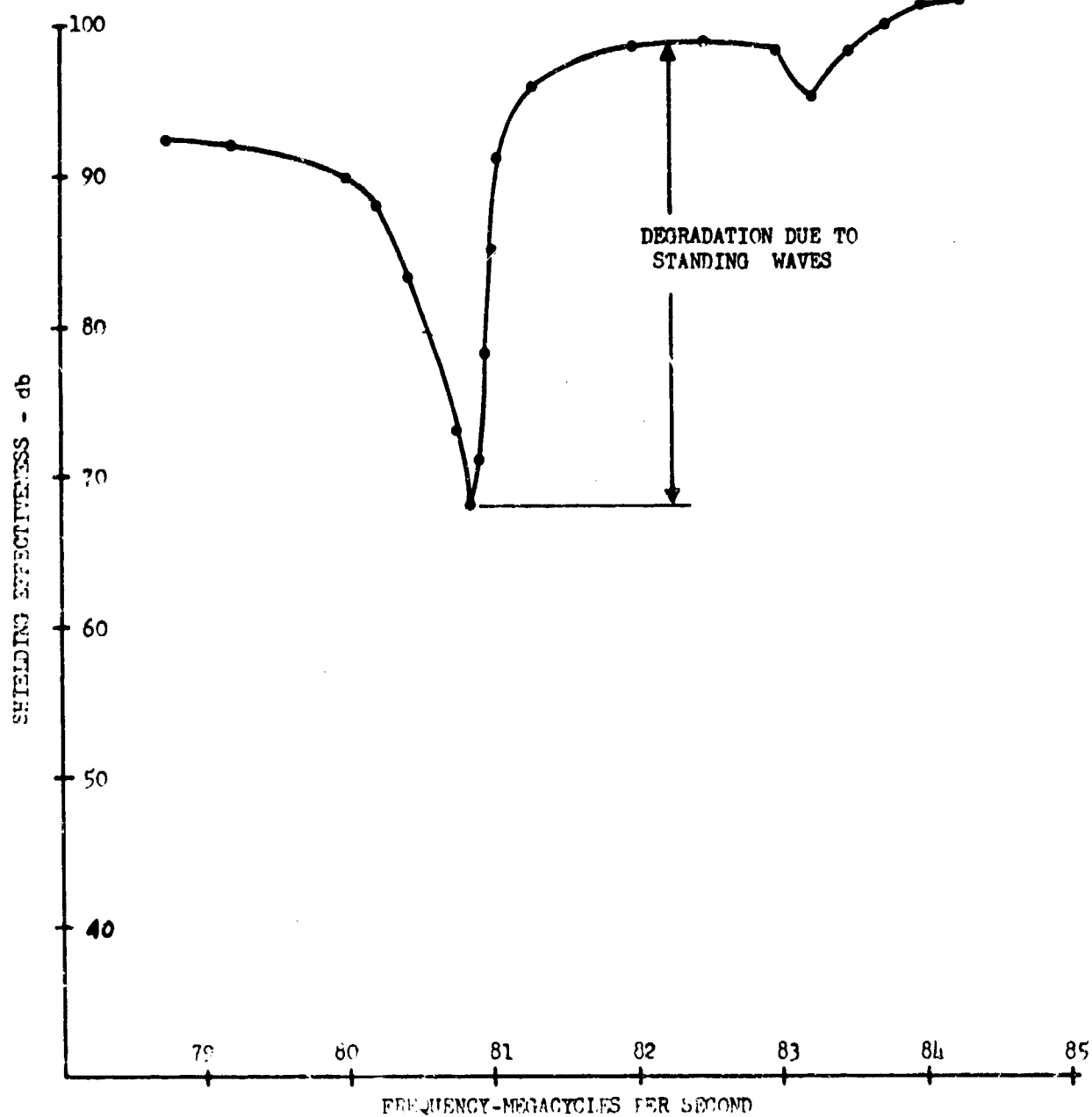
FIG. 8 VARIATION OF SHIELDING EFFECTIVENESS
OF CELL-TYPE ENCLOSURE NEAR THE
LOWEST NATURAL RESONANT FREQUENCY
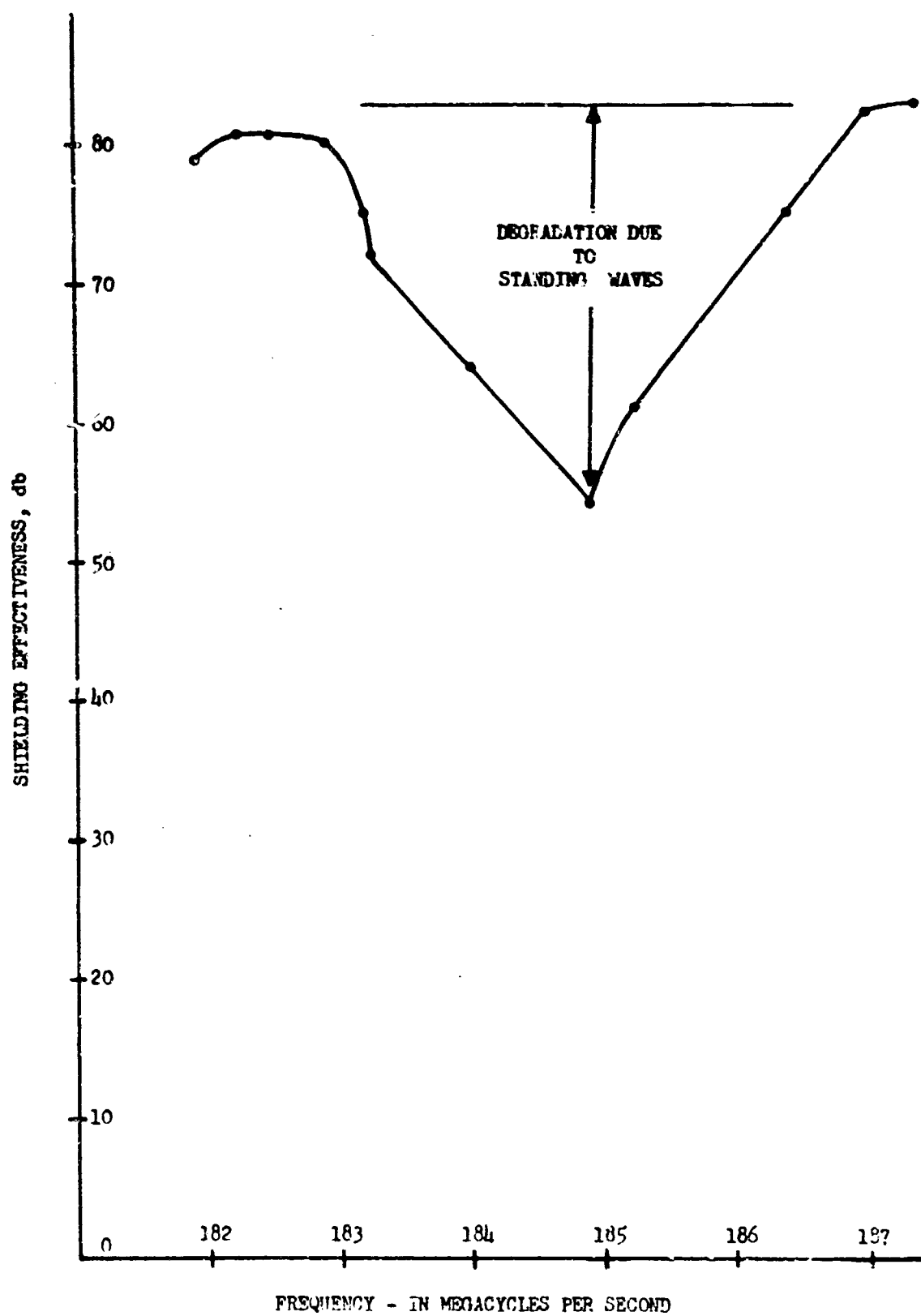
FIG. 9   VARIATION OF SHIELDING EFFECTIVENESS OF CELL-TYPE
ENCLOSURE NEAR THE RESONANT FREQUENCY OF 184 mc.

- 28 -

NO POINTS WERE TAKEN
BETWEEN POINTS JOINED
WITH DOTTED LINE.

DEGRADATIONS INTRODUCED
BY THE PRESENCE OF
STANDING WAVES AT THE
NATURAL RESONANT FREQUENCIES

FREQUENCY - MEGACYCLES PER SECOND

SHIELDING EFFECTIVENESS - db

FIG. 10 SHIELDING EFFECTIVENESS OF A CELL-TYPE ENCLOSURE
TO PLANE WAVE IMPEDANCE FIELDS

- 27 -

appreciably (1) as the reviewed frequency sweeps past the resonance frequency during measurements and (2) when the antenna is taken outside the enclosure, as does the impedance of the half-wave dipole antenna[1].

The output of antenna A_1 was brought outside the enclosure to an IM-88/URM-47 Radio Interference/Field Intensity Meter through a coaxial feed-through connector located in the roof of the enclosure. In order to minimize unwanted pick-up and field distortion, cable C_3 was kept as short as possible; RG/U-9B double shielded cable was used. The presence of excessive leakage at the ri/fi meter necessitated the construction of a shielded case for the meter. Cable C_3 was also provided with a third shield. When the connectors C or C' were shorted out, it was found that the meter was not picking up any stray fields. The antenna A_1 inside the shielded enclosure where the electric field intensity was high was supported by its tripod. (In case of the lowest natural resonant frequency, the electric field intensity is maximum at the center of the enclosure and its orientation is perpendicular to the plane of the largest side panel.)

The transmitting antenna A_2 was oriented perpendicular to the center of the largest wall of the enclosure[2] and was pulled away until a maximum indicatio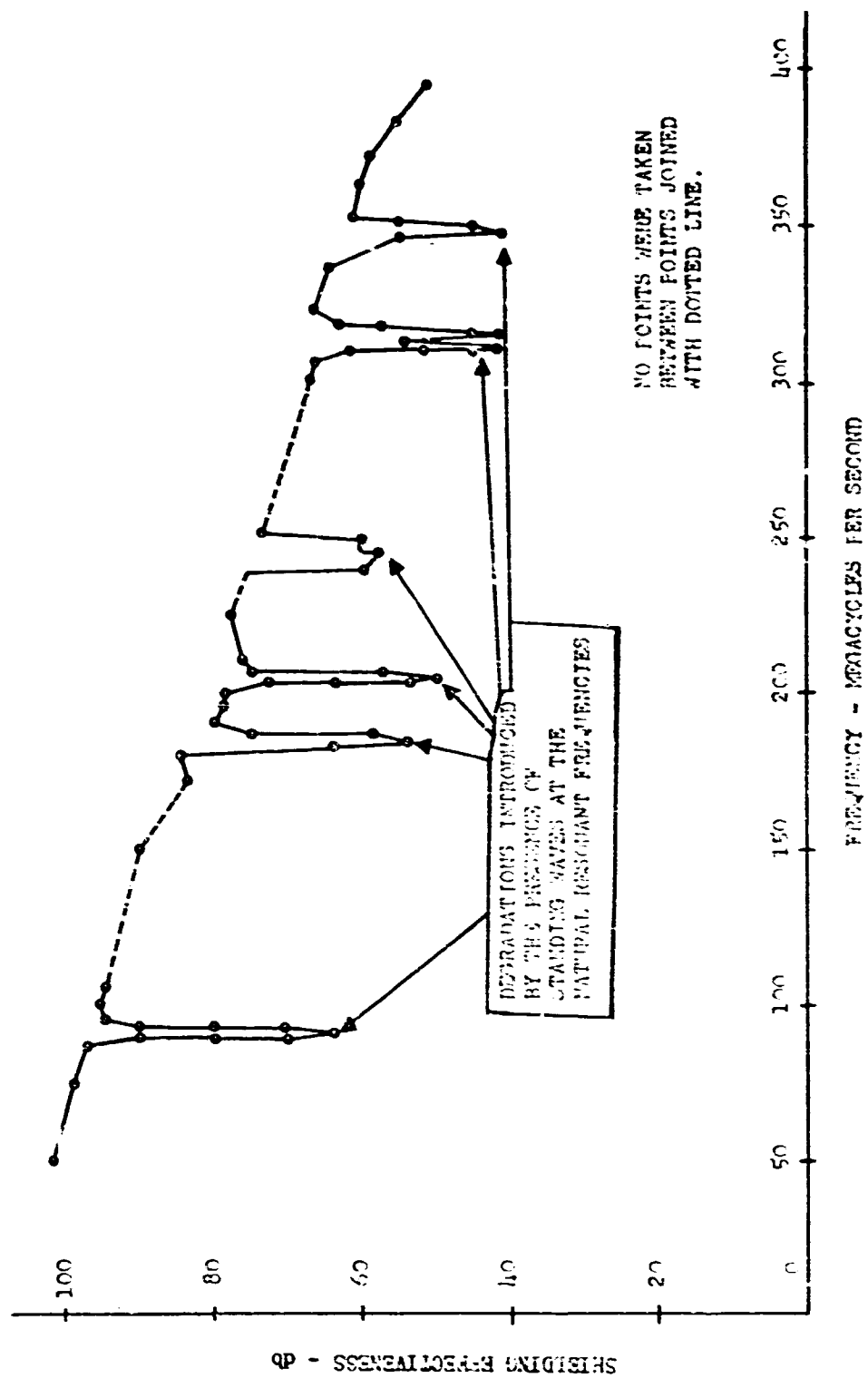n was obtained at the meter M. This distance of the center of the antenna A_2 from the enclosure wall corresponds to an integral multiple of half wave-lengths $(n \frac{\lambda}{2})$. However, to prevent interaction of A_2 with the enclosure walls, n was kept greater than 3. The generator frequency was varied in very small steps around the resonant frequency and curves were plotted similar to the ones which appear in Figures 8, 9, and 10. The coupling of the antennas A_1 and A_2 was also measured outside the enclosure when spaced the same distance and oriented the same way as when one was inside and the other outside. The

---

[1] Reference 2, pp. 36-37.
[2] This orientation will favor the TE_{101} mode of excitation.

ARMOUR RESEARCH FOUNDATION OF ILLINOIS INSTITUTE OF TECHNOLOGY

ARF Proj. E108
Quar. Rpt. No. 4

shielding effectiveness at the lowest natural resonant frequency is defined as the increase in attenuation of the output generator G to give the same reading indication on the meter M that existed for reception through the enclosure shield.

It should be mentioned at this point that the position of the receiving antenna A_1 in the center of the enclosure is exactly correct with respect to the orientation and location of the maximum electric field in the cavity only for the case of the lowest natural resonant frequency. Although the location and direction of the maximum electric field changes within the cavity with the various natural resonant frequencies, the tests performed to take the data which appear in Figures 9 and 10 had the antenna A_1 always in the same position, the center of the enclosure.

If the antenna location is changed within the enclosure, the pick-up voltage will also be changed. The measurements are also subject to the test conditions; that is, any metallic objects present inside or outside the enclosure may affect the measurement results. Metallic objects or other perturbations placed inside the enclosure at points where the magnetic field is maximum have the effect of increasing the resonant frequency (from the calculated value); when placed at points where the electric field is maximum they have the effect of reducing the value of the calculated resonant frequency[1]. In the case of the first resonant frequency, for example, the dipole antenna A_1 and its supporting structure, since it is placed at the center of the enclosure where the electric field is maximum, reduced the value of the resonant frequency from the calculated value of 83.4 mc to the measured value of 80.85 mc. Losses present in the walls, by the same token, increase or reduce the values of the resonant

[1]Reference 6, pp. 80-81.

frequencies if the magnetic or electric field is maximum at those locations.

In addition, the resonant frequencies crowd together as one goes up in frequency, and their effects overlap. To keep the test as simple as possible, it is proposed that the test for shielding effectiveness be performed at the lowest natural resonant frequency of the enclosure when it is considered as a cavity.

3. Conclusions

For the enclosure tested, the shielding effectiveness to plane-wave-impedance fields at mid-frequencies varies from about 100 db at 60 mc to about 65 db at 400 mc. The reduction in shielding effectiveness at the narrow peaks of the natural resonant frequencies is about 25 to 30 db and brings the field intensity value inside the shielded enclosure well within the sensitivity range of the ri/fi instruments now used. However, the shielding effectiveness to plane-wave impedance fields offered by solid sheets of copper of a few thousandths of an inch thick is much higher than screening material. Therefore, a test for resonant frequencies might be quite difficult under these conditions.

Nevertheless, it is planned that a test of this type will be included in the revised test standards for measuring shielding effectiveness of shielded enclosures since the data are important to the description of shielding effectiveness.

D. High-Frequency Tests

The testing of the enclosure in the neighborhood of 9 kilomegacycles has temporarily been delayed because of a failure of the AN/APS-25 radar unit which was employed as a high power source.

B. Coaxial Testing Device

1. Introduction

In the Second and Third Quarterly Progress Reports, it was indicated
that a section of coaxial transmission line could be used to measure the shield-
ing effectiveness of materials to plane waves. A thin lamina of the material
is inserted in the line as a barrier extending from the inner to the outer
coaxial conductors and perpendicular to them as in Figure 11(a). It was shown
in the Third Quarterly Progress Report that the portion of the coaxial guide
filled with the shielding material under test can be represented as a trans-
mission line whose per-unit impedance and admittance are given by

$$(44) \qquad Z = \frac{j\omega\mu \ell n \frac{b}{a}}{2\pi} \quad \text{ohms/meter}$$

and

$$(45) \qquad Y = \frac{\sigma \, 2\pi}{\ell n \frac{b}{a}} \quad \text{mho/meter,}$$

respectively. This transmission line portion is shown in Figure 11(b).

2. Equivalent Circuit of the Transmission Line

It is desirable to construct a lumped four-terminal network whose
external behavior will simulate that of the given line of length d which repre-
sents the lamina. The impedance matrix for a transmission line of length d is[1]

$$(46) \qquad \underline{Z} = \frac{\mathcal{Z}_\ell}{\sinh \gamma d} \begin{pmatrix} \cosh \gamma d & 1 \\ 1 & \cosh \gamma d \end{pmatrix},$$

where

$$(47) \qquad \mathcal{Z}_\ell = \sqrt{\frac{Z}{Y}} = (1 + j) \frac{\ell n \frac{b}{a}}{2\pi} \sqrt{\frac{\omega\mu}{2\sigma}},$$

---

[1] Reference 3, pp. 256-276.

ARF Proj. E108
Quar. Rpt. No. 4

RADIUS OF OUTER CONDUCTOR , b

d

$\mu_0, \epsilon_0, \sigma_0 = 0$

RADIUS OF INNER CONDUCTOR, a

BARRIER OF THICKNESS, d
μ, ϵ, σ

(a) CROSS SECTIONAL VIEW

$$\gamma = (1+j)\sqrt{\frac{\omega\mu\sigma}{2}}$$

$$Z_2 = (1+j)\frac{Ln\frac{b}{a}}{2\pi}\sqrt{\frac{\omega\mu}{2\sigma}} \qquad ; \quad d$$

(b) EQUIVALENT TRANSMISSION LINE OF LAMINA

ONE T — (n−1) T's

$\frac{L\ell}{2n}$ $\frac{L\ell}{2n}$ $\frac{L\ell}{2n}$ $\frac{L\ell}{2n}$ $\frac{L\ell}{2n}$

$\frac{Z_1}{2}$ $\frac{Z_1}{2}$

Z_2 $nR\ell$ $nR\ell$ $nR\ell$
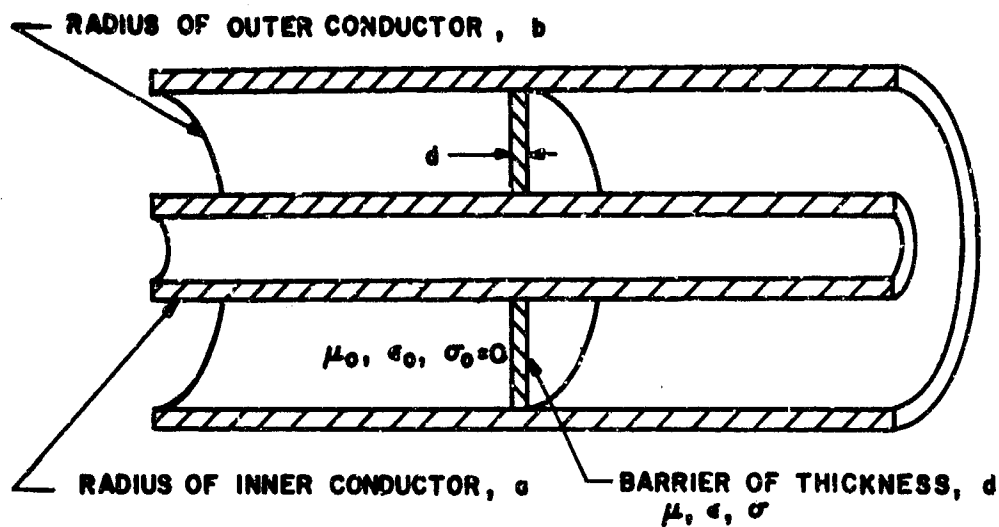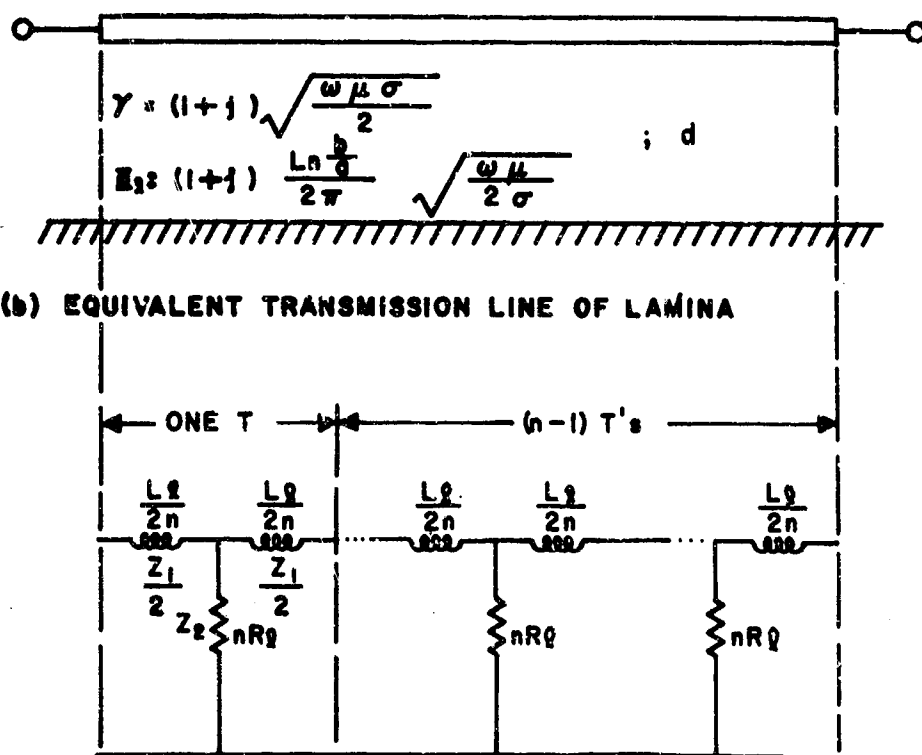
(c) ARTIFICIAL LINE COMPOSED OF n IDENTICAL T's

FIG. II COAXIAL TESTING DEVICE

and

$$(48) \qquad \gamma = \sqrt{ZY} = (1 + j)\sqrt{\frac{\omega\mu\sigma}{2}}$$

are the characteristic impedance and propagation constant, respectively, of
the transmission line that represents the lamina.

The transmission line shown in Figure 11(b) can be realized over a
band of frequencies with a number of simple T's as shown in Figure 11(c), for
which

$$(49) \qquad z_1 = \frac{d}{n} \; j\omega\mu \; \frac{\ell n \frac{b}{a}}{2\pi} \;,$$

$$(50) \qquad \frac{1}{z_2} = \frac{d}{n} \; \sigma \; \frac{2\pi}{\ell n \frac{b}{a}} \;,$$

and n is the number of simple T's employed. The characteristic impedance of
the cascaded n T's must be the same as that of the transmission line they
represent, namely $\mathbf{Z}_\ell$, and the propagation functions must be the same; thus,[1]

$$(51) \qquad \mathbf{Z}_T = \sqrt{z_1 z_2} \; \sqrt{1 + \frac{z_1}{4z_2}} = \mathbf{Z}_\ell \sqrt{1 + \left(\frac{\gamma d}{2n}\right)^2} = \mathbf{Z}_\ell$$

$$(52) \qquad n\gamma_T = 2n \sinh^{-1} \sqrt{\frac{z_1}{4z_2}} = 2n \sinh^{-1} \left(\frac{\gamma d}{2n}\right) = \gamma d.$$

Expand (51) with the binomial theorem and use for (52) the expansion

$$(53) \qquad \sinh^{-1} = u - \frac{1}{2} \frac{u^3}{3} + \frac{1}{2} \frac{3}{4} \frac{u^5}{5} - \cdots$$

for small u to get

$$(54) \qquad Z_T = \mathbf{Z}_\ell \left\{ 1 + \frac{1}{2} \left(\frac{\gamma d}{2n}\right)^2 - \frac{1}{8} \left(\frac{\gamma d}{2n}\right)^4 + \cdots \right\},$$

---

[1] Reference 3, p. 258.

$$(55) \quad n\gamma_T = \gamma d \left\{ 1 - \frac{1}{6} \left(\frac{\gamma d}{2n}\right)^2 + \frac{3}{40} \left(\frac{\gamma d}{2n}\right)^4 - \cdots \right\}.$$

If $\frac{d}{n}$ is chosen in such a way that the fourth power terms in (54) and (55) are much smaller than the square terms, one can determine the number of sections necessary to give a certain amount of error in Z_ℓ and γ.

Thus, from Equations (54) and (55), one may define

$$(56) \quad \sum_{Z_\ell} = \frac{1}{2} \left(\frac{\gamma d}{2n}\right)^2 Z_\ell \quad \text{as the error in } Z_\ell$$

and

$$(57) \quad \sigma_\gamma = \frac{1}{6} \left(\frac{\gamma d}{2n}\right)^2 \gamma \quad \text{as the error in } \gamma.$$

To determine the required number n of T's, assume a 5 percent allowable error in the characteristic impedance; thus

$$(58) \quad 0.05 \geq \frac{1}{8} \left| \frac{\gamma d}{n} \right|^2$$

For the case of copper and $f = 5 \times 10^6$, $d = 2.5$ mils $= 6.35 \times 10^{-5}$ meters,

$$(59) \quad n \geq 1.5 .$$

Hence, two T's will suffice to represent the lamina whose total inductance and resistance are

$$(60) \quad L_\ell = 10.6 \times 10^{-12} \text{ henry}$$

and

$$(61) \quad R_\ell = 50 \times 10^{-6} \text{ ohms,}$$

respectively, up to the frequency of 5×10^6 cps. The single-T representation of the lamina which was given in the Third Quarterly Progress Report is too gross an approximation, except at the lowest frequencies. The two-T representation, on the other hand, is valid up to a frequency near 10^7 cps. Figure 12
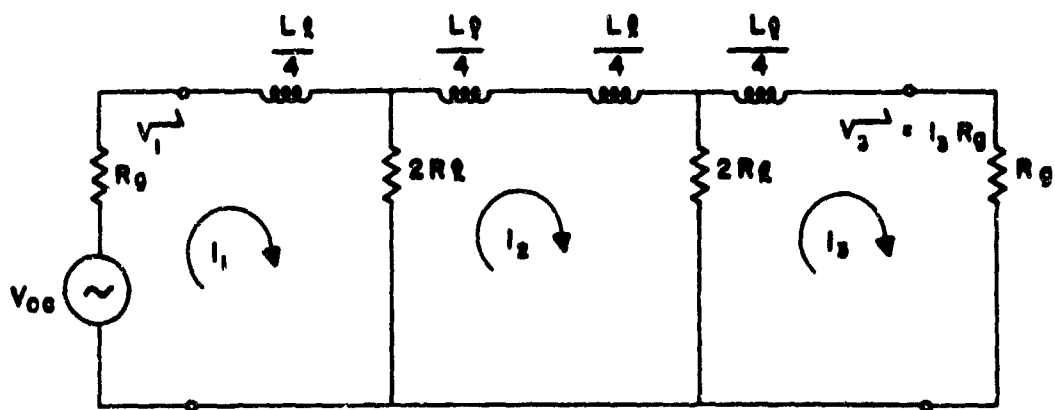
R_g — GENERATOR IMPEDANCE = $50\,\Omega$

R_ℓ — TOTAL LAMINA RESISTANCE = $50 \times 10^{-6}\,\Omega$

L_ℓ — TOTAL LAMINA INDUCTANCE = 10.6×10^{-12} HENRY

SHIELDING EFFECTIVENESS (DECIBELS) = $20 \, LOG \left| \dfrac{V_1^\rightarrow}{V_3^\rightarrow} \right|$

FIG. 12 EQUIVALENT CIRCUIT OF THE COPPER LAMINA

represents a two-T network representation of the copper lamina. Solving for I_3 by loop currents, one gets, by noting that $R_\ell \ll R_g$ and $\omega L_\ell \ll R_g$,

$$(62) \qquad I_3 = \frac{V_{oc} R_\ell^2}{R_g^2 (R_\ell + j\frac{\omega L_\ell}{8})}$$

and

$$(63) \qquad V_3 = I_3 R_g = \vec{V_3} = \frac{V_{oc} R_\ell^2}{R_g (R_\ell + j\frac{\omega L_\ell}{8})} .$$

The symbol $\vec{V_3}$ is used to designate a voltage wave propagated in the positive (incident) direction in loop 3. The shielding effectiveness is defined in this application as

$$(64) \qquad S. E. (db) = 20 \log \left| \frac{\vec{V_1}}{\vec{V_3}} \right| .$$

Substituting Equation (63) into Equation (64), one gets, noting that $\vec{V_1} = \frac{V_{oc}}{2}$,

$$(65) \qquad S. E. (db) = 20 \log \frac{R_g \sqrt{1 + (\frac{\omega L_\ell}{8 R_\ell})^2}}{2 R_\ell}$$

Equation (65) reduces in the low-frequency limit to the expression

$$(66) \qquad \lim_{\omega \to 0} S. E. = 20 \log \frac{R_g}{2 R_\ell} ,$$

which may be obtained from Figure 12 by letting L_ℓ go to zero as ω goes to zero, and then solving for the ratio appearing in Equation (66).

3. Experimental Results

The set-up shown in Figure 13 was used to take the coaxial tester experimental data which are plotted in Figure 14 for a lamina thickness of 2.5 mils. The shielding effectiveness is much higher than the sensitivity of
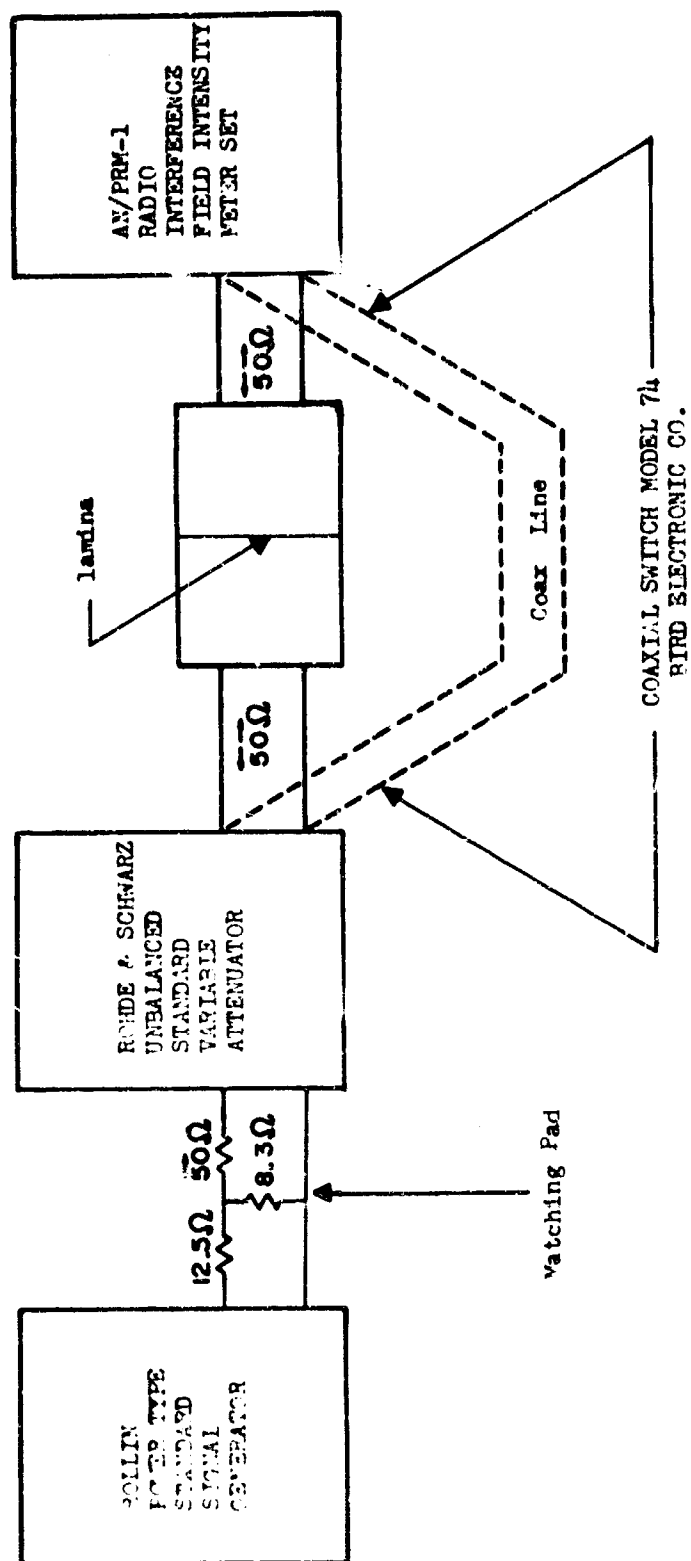
FIG. 13 EXPERIMENTAL SETUP FOR MEASURING SHIELDING EFFECTIVENESS WITH THE COAXIAL TESTING DEVICE

FIG. 14 SHIELDING EFFECTIVENESS TO PLANE WAVES OF SHEET COPPER

SHEET COPPER
d = 2.3 MILS
RELATIVE PERMEABILITY $\mu_r = 1$
RESISTIVITY $\rho = 1.76 \times 10^{-8}$ OHM-METER
$R_\ell = 50 \times 10^{-6}$ OHM
$L_\ell = 10.6 \times 10^{-12}$ HENRY

(a) ―●― TRANSMISSION LINE THEORY
(b) ―●― CIRCUIT EQUIVALENT OF (a)
(c) ―●― EXPERIMENTAL DATA

FREQUENCY – CYCLES PER SECOND

SHIELDING EFFECTIVENESS – DECIBELS

- 64 -

the instruments to detect beyond 5 mc. On the same figure, the calculated shielding effectiveness from equation (65) is also plotted.

The experimental points are taken as follows: (1) With 20 db attenuation in the variable attenuator for isolation, observe an indication on the field intensity meter when the signal passes through the coaxial testing device. (2) Insert enough additional attenuation in the variable attenuator until the same indication as in (1) is observed on the field intensity me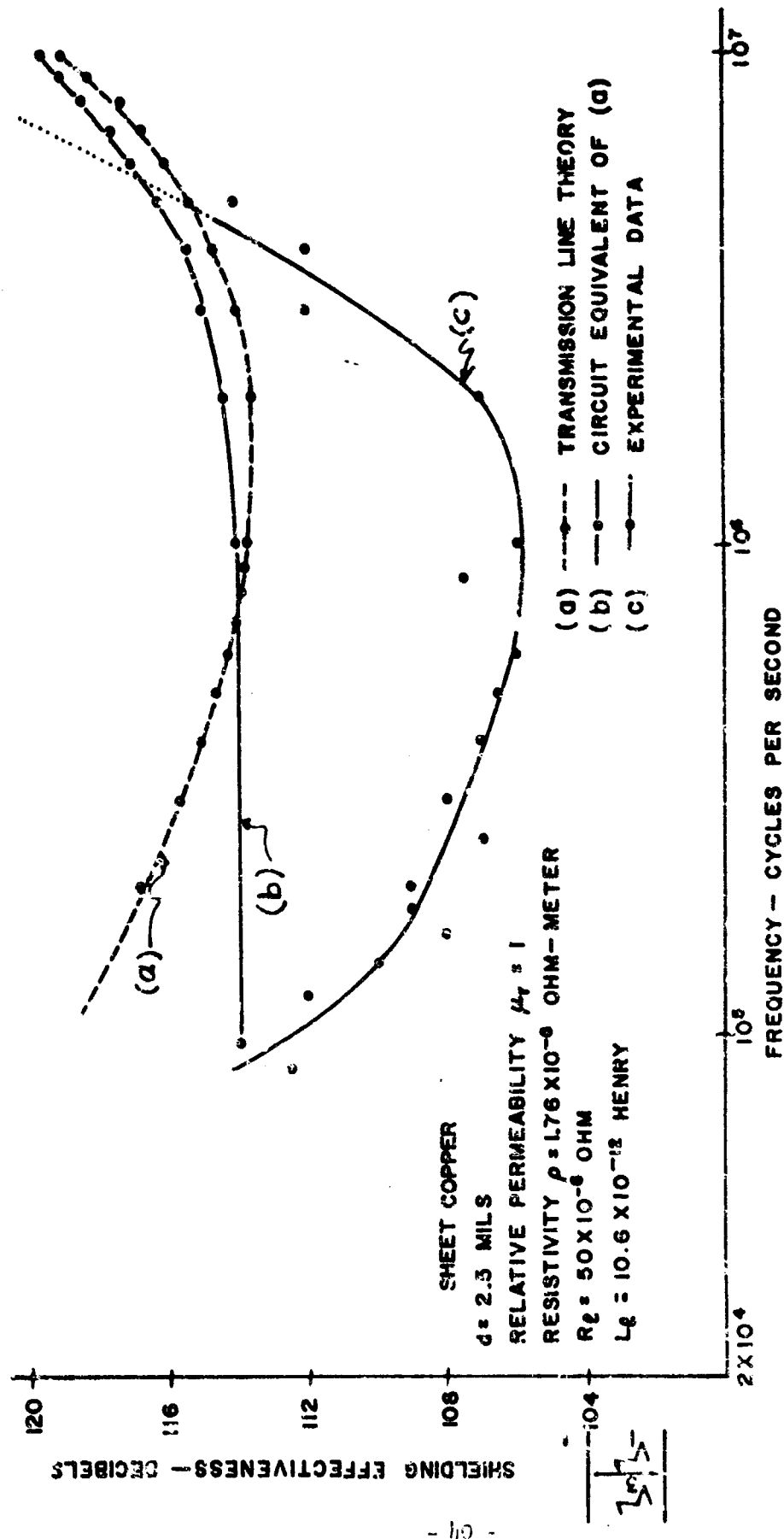ter when the signal is directly fed to that meter by the use of two coaxial switches (see dotted lines in Figure 13). The increase in db attenuation introduced by the variable attenuator is the shielding effectiveness of the lamina.

It is believed that the experimental curve does not follow the calculated curve for shielding effectiveness because of the generation of higher modes in the lamina. These higher modes when generated at the surface of the lamina are attenuated, especially at those frequencies at which the lamina thickness, d, becomes an appreciable portion of the wavelength, and thus introduce additional loss. The higher modes are generated because (1) the contact resistance in the lamina is non-uniform, (2) the lamina has surface irregularities, and (3) the wavelength of the electromagnetic waves in the lamina is quite small. Conditions (1) and (2) produce a non-uniform surface current distribution which requires higher modes to satisfy its boundary conditions at the surface of the lamina. The consequence of condition (3) is to increase the effective dimensions of the lamina diameter and width by many times over the corresponding dimensions in air; the lamina space then can support the higher modes generated under conditions (1) and (2) in addition to other higher modes generated under condition (3).

To illustrate, the wavelength of electromagnetic waves in the TEM mode at a frequency of one megacycle is

$$(67) \qquad \lambda_0 = \frac{c}{f} = \frac{3 \times 10^6}{10^6} = 300 \text{ meters}$$

The propagation constant in a good conductor is

$$(68) \qquad \gamma = \alpha + j\beta = (1 - j)\sqrt{\frac{\omega\mu\sigma}{2}} \ ,$$

and the following relationship holds

$$(69) \qquad \lambda = \frac{2\pi}{\beta} \ .$$

The wavelength of the electromagnetic waves at $f = 10^6$ in copper ($\mu = 4\pi \times 10^{-7} \frac{h}{m}$, $\sigma = 5.75 \times 10^7 \frac{mho}{m}$), is

$$(70) \qquad \lambda_{cu} = \frac{2\pi}{\sqrt{\frac{\omega\mu\sigma}{2}}} = 416 \ \mu \text{ meters}$$

and that in high-μ metal at the same frequency ($\mu = 1.6\pi \times 10^{-3}$ h/m, $\sigma = 1.12 \times 10^6$ mho/m) is

$$(71) \qquad \lambda_{high-\mu} = \frac{2\pi}{\sqrt{\frac{\omega\mu\sigma}{2}}} = 46.7 \ \mu \text{ meters}.$$

Since $d_{cu} = 2.5$ mils $= 6.35 \times 10^{-5}$ meter $= 63.5 \ \mu$ meters and $d_{high-\mu} = 3.5$ mils $= 8.9 \times 10^{-5}$ meter $= 89 \ \mu$m, one has

$$(72) \qquad \frac{d}{\lambda}\bigg|_{copper} = .152 \text{ and } \frac{d}{\lambda}\bigg|_{high-\mu \ metal} = 1.9.$$

At $f = 2.7 \times 10^6$ cps in the case of copper and at $f = 1.74 \times 10^3$ cps for the case of the high-μ metal,

(73) $\qquad \dfrac{d}{\lambda} = \dfrac{1}{4}$

and the laminas appear to be a quarter of a wavelength thick.

Thus the wavelength in the conducting material is reduced by

(74) $\qquad \dfrac{\lambda_o}{\lambda_{cu}} = \dfrac{300}{416} \ 10^6 = 72 \times 10^6$ times for the copper lamina

and

(75) $\qquad \dfrac{\lambda_o}{\lambda_{high\ -\mu}} = \dfrac{300}{46.7} \ 10^6 = 6.42 \times 10^6$ times for the high-μ metal lamina.

Thus, in the case of the high-μ metal, and for the same error of 0.05, the 3.5-mil lamina requires an artificial line representation consisting of 700 simple T's for frequencies up to one megacycle; therefore it is not helpful to analyze it from that point of view. In a later paragraph, the transmission line analogy is analyzed and compared with experiment.

Figure 15 shows the shielding effectiveness of high-μ metal (nominal $\mu_r = 10^4$), 3.5 mils thick. The sensitivity of the instruments limit the measurement range to 650 kilocycles. Figure 16 shows the shielding effectiveness of 5-mil thick aluminum and Figures 17 and 18 that of 18-mil thick stainless steel and 5-mil thick magnetic steel, respectively. Figure 19 shows the shielding effectiveness of copper screening material (22 x 22 strands per inch, 15 mils diameter) of one shielding enclosure manufacturer. The effectiveness at very low frequencies is primarily due to reflection and the effect of perforations does not come into play until the higher frequencies, where the shielding effectiveness drops with frequency.
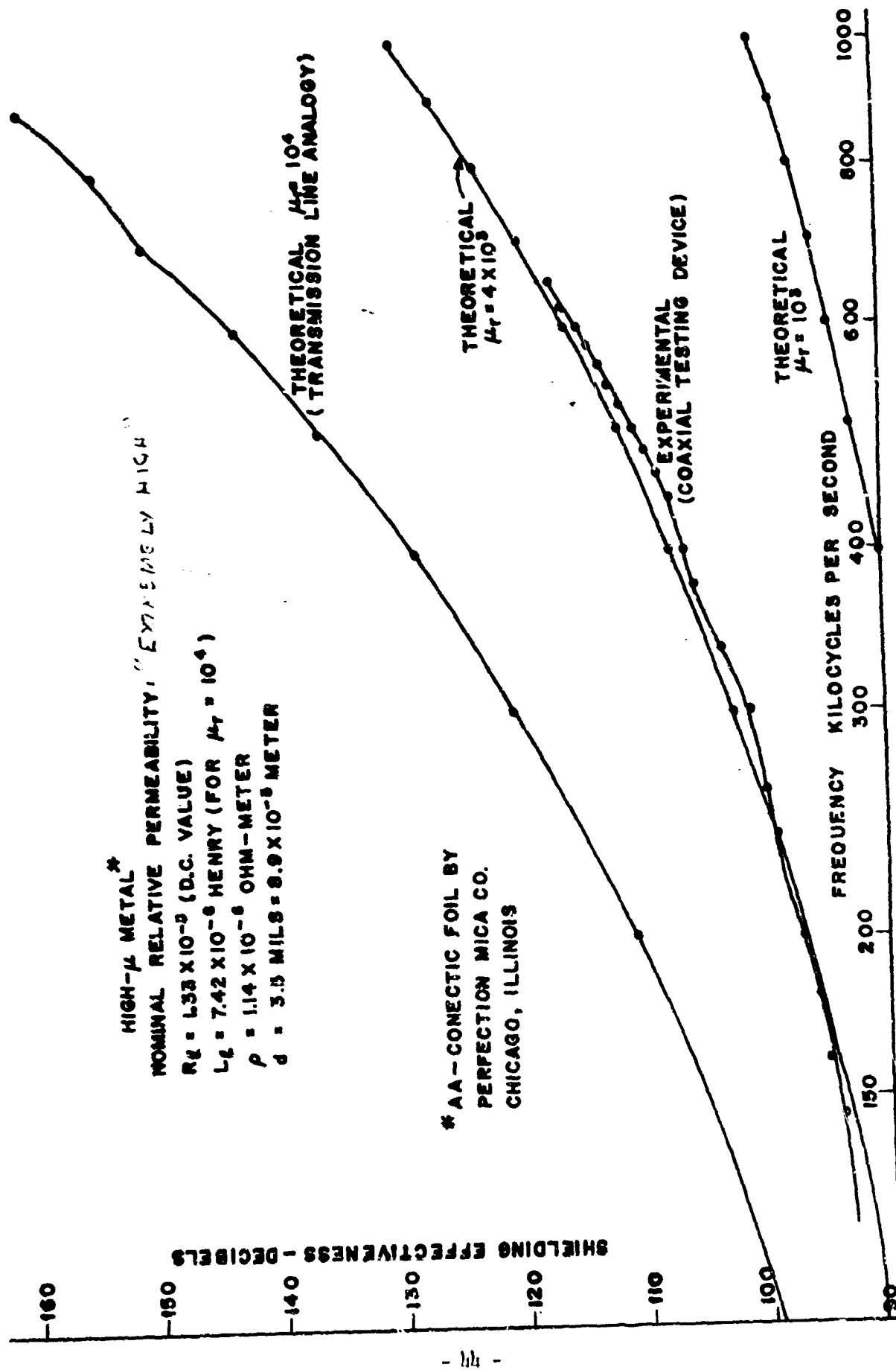
FIG. 15 SHIELDING EFFECTIVENESS TO PLANE WAVES OF HIGH-μ METAL

HIGH-μ METAL*
NOMINAL RELATIVE PERMEABILITY: "EXTREMELY HIGH"

$R_L = 1.38 \times 10^{-3}$ (D.C. VALUE)
$L_L = 7.42 \times 10^{-8}$ HENRY (FOR $\mu_r = 10^4$)
$\rho = 1.14 \times 10^{-6}$ OHM-METER
$d = 3.5$ MILS $= 8.9 \times 10^{-5}$ METER

*AA—CONECTIC FOIL BY
PERFECTION MICA CO.
CHICAGO, ILLINOIS

THEORETICAL $\mu_r = 10^4$
(TRANSMISSION LINE ANALOGY)

THEORETICAL
$\mu_r = 4 \times 10^3$

EXPERIMENTAL
(COAXIAL TESTING DEVICE)

THEORETICAL
$\mu_r = 10^3$

FREQUENCY KILOCYCLES PER SECOND

SHIELDING EFFECTIVENESS — DECIBELS

- 44 -

ALUMINUM

PERMEABILITY $\mu_{AL} = \mu_o = 4\pi \times 10^{-7}$ HENRY/METER

THICKNESS OF LAMINA $d = 5$ MILS

$R_L = 57 \times 10^{-6}$ OHM $= 57 \mu\Omega$

SHIELDING EFFECTIVENESS – DECIBELS

120   115   110   105   100

.2   .4   .6   1.   2.   4.   6.

FREQUENCY – MEGACYCLES PER SECOND

FIG. 16   SHIELDING EFFECTIVENESS TO PLANE WAVES OF ALUMINUM

- 45 -

STAINLESS STEEL
THICKNESS= 18 MILS
RELATIVE PERMEABILITY $\mu_r = 1$
RESISTIVITY $\rho = 7.35 \times 10^{-5}$ OHM-CM
RESISTANCE OF LAMINA $R_L = 240\mu\Omega$
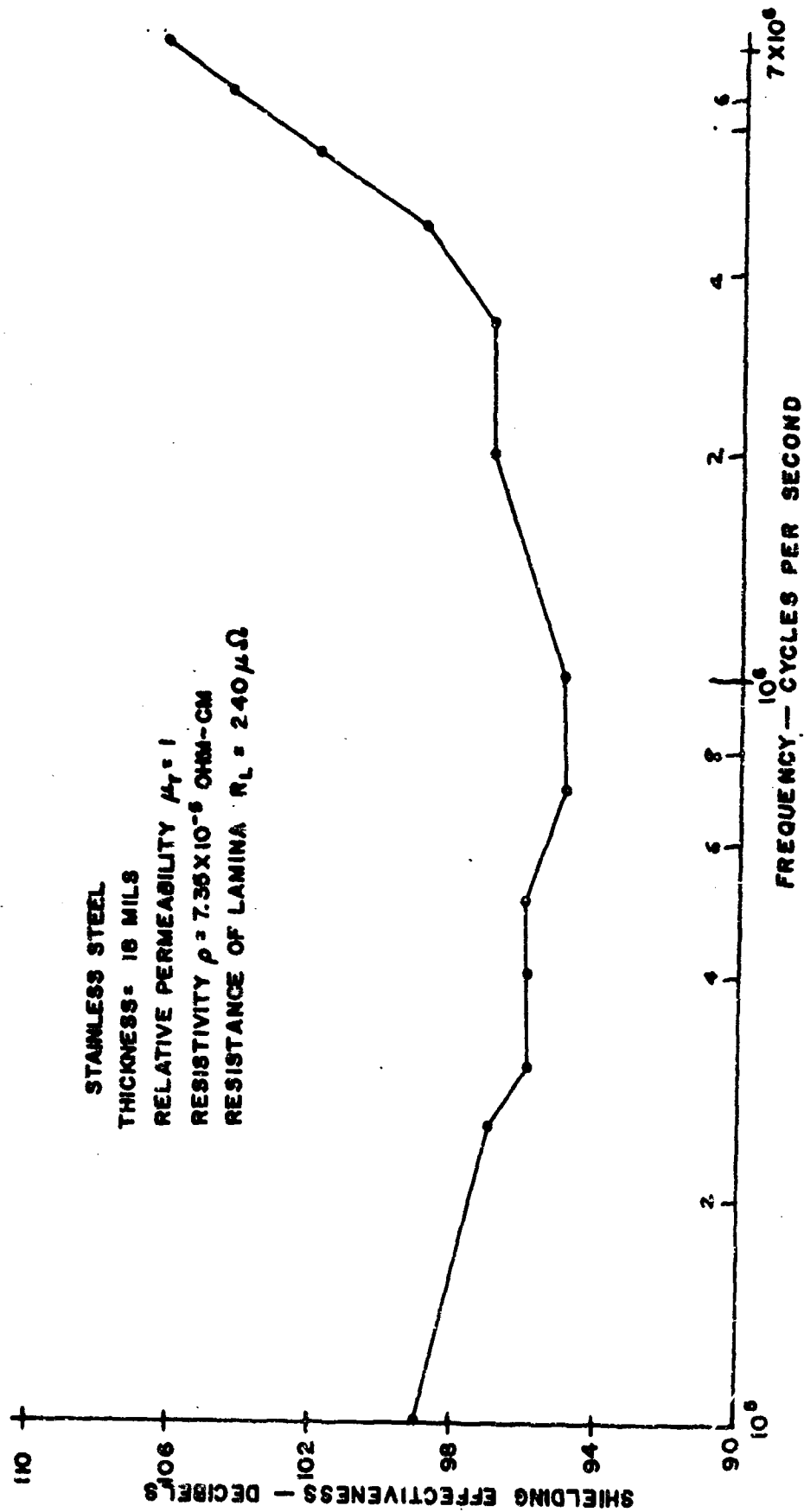
FIG. 17 SHIELDING EFFECTIVENESS TO PLANE WAVES OF STAINLESS STEEL

MAGNETIC STEEL

d = 4.5 MILS

RELATIVE PERMEABILITY $\mu_r = 250$

RESISTIVITY $\rho = 59 \times 10^{-8}$ OHM-METER
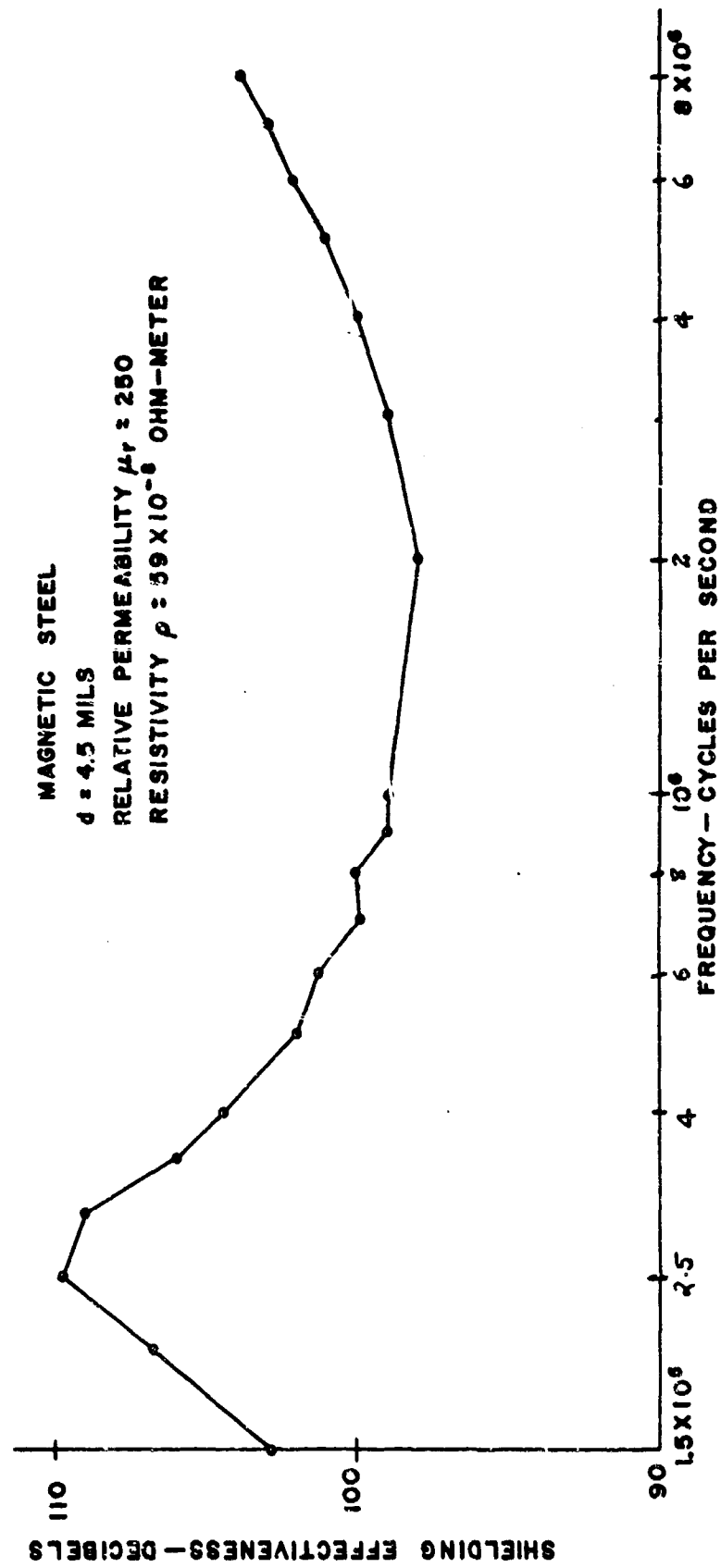
FIG. 18   SHIELDING EFFECTIVENESS TO PLANE WAVES OF MAGNETIC STEEL

COPPER SCREENING
22 X 22 STRANDS PER INCH,
EACH STRAND 15 MILS DIAMETER

TO 150 db at d.s.

SHIELDING EFFECTIVENESS — DECIBELS
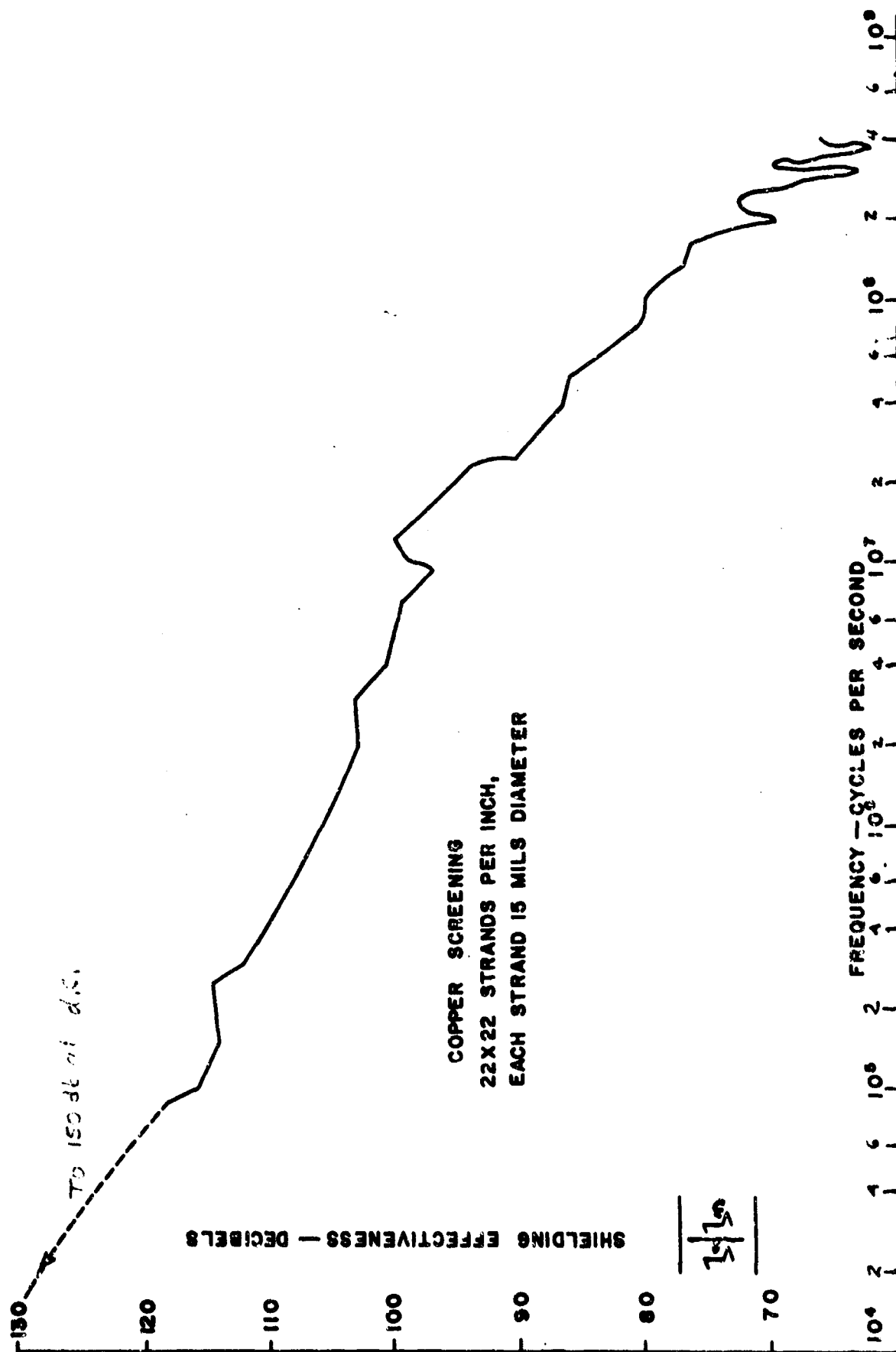
FREQUENCY — CYCLES PER SECOND

FIG. 19 SHIELDING EFFECTIVENESS TO PLANE WAVES OF ONE LAYER OF COPPER SCREENING

4. Transmission Line Analogy

In the case of the high-μ metals (such as iron) and other metals whose lamina thickness appears to be many wavelengths, the transmission line analogy may be used. In this case, the lamina is considered as a transmission line of characteristic impedance

$$(76) \qquad Z_\ell = (1 + j) \; \frac{\ln \frac{a}{b}}{2\pi} \; \sqrt{\frac{\omega\mu}{2\sigma}}$$

and propagation constant

$$(77) \qquad \gamma = (1 + j)\sqrt{\frac{\omega\mu\sigma}{2}} = \alpha + j\beta$$

sandwiched between two transmission lines of characteristic impedance

$$(78) \qquad Z = 50 \text{ ohms}$$

and propagation constant

$$(79) \qquad \gamma_o = j\,\beta_o = j\,\frac{2\pi}{\lambda_o}$$

where λ_o is the wavelength of the TEM mode of frequency f_o. Multiple reflections in the transmission line representing the lamina are neglected since the attenuation is considered to be so high as to reduce them appreciably. Thus, at the junction (1) see Figure 20(A)

$$(80) \qquad \vec{V_1} + \overleftarrow{V_1} = \vec{V_2}$$

and

$$(81) \qquad \vec{I_1} - \overleftarrow{I_2} = \vec{I_2} \;.$$

But

$$(82) \qquad \vec{V} = Z \; \vec{I} \;.$$
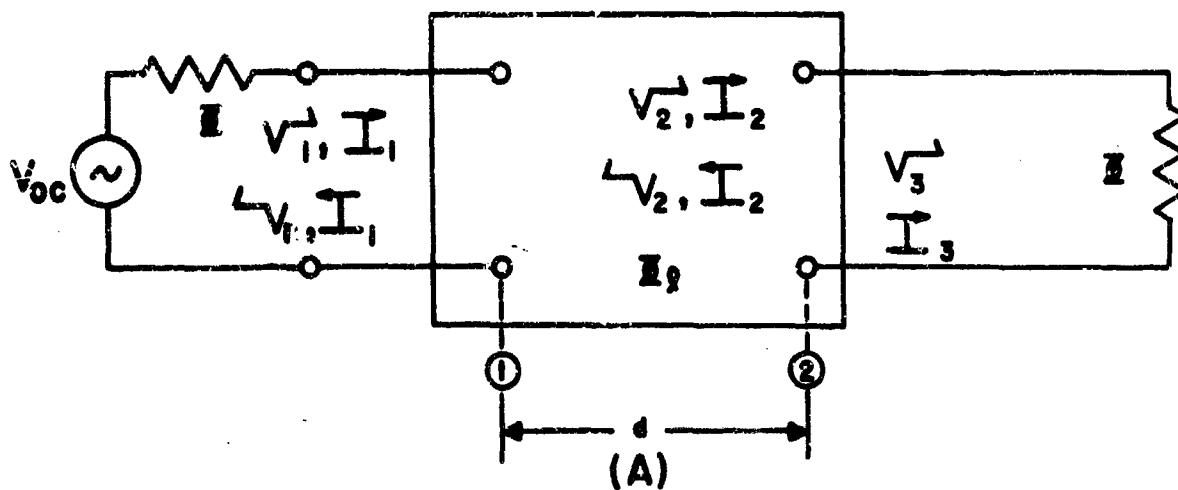
FORWARD TRAVELING VOLTAGE WAVE AMPLITUDE

BACKWARD TRAVELING VOLTAGE WAVE AMPLITUDE

FORWARD TRAVELING CURRENT WAVE AMPLITUDE

BACKWARD TRAVELING CURRENT WAVE AMPLITUDE

FIG. 20   TRANSMISSION LINE REPRESENTATION OF COAXIAL TESTING DEVICE

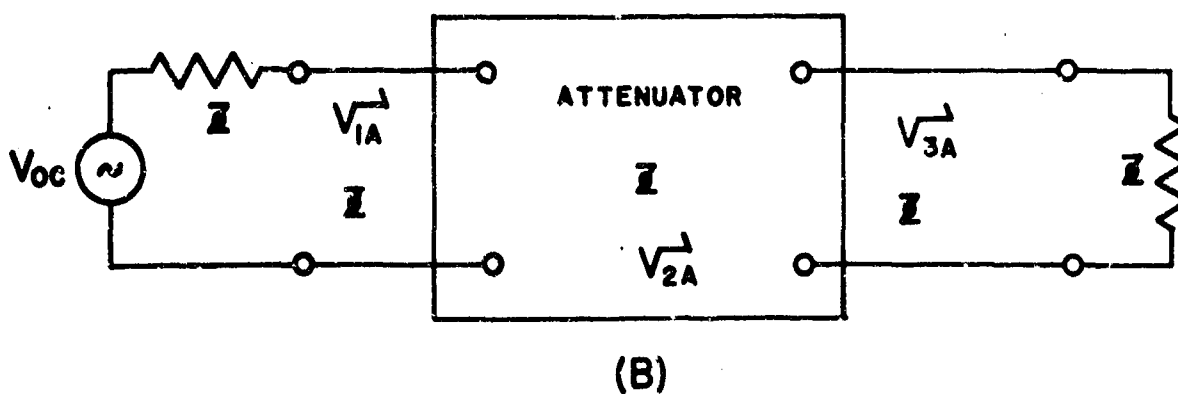Thus (81) becomes, with the use of (82),

$$(83) \qquad \vec{V_1} - \overleftarrow{V_1} = \mathbf{z} \; \frac{z_\ell}{z_\ell} \vec{I_2} = \frac{z}{z_\ell} \vec{V_2} \quad .$$

Adding (80) and (83) and dividing by 2, one gets

$$(84) \qquad V_1 = \frac{1}{2} \left(1 + \frac{z}{z_\ell}\right) \vec{V_2} \quad .$$

At junction (2), see Figure 20(A),

$$(85) \qquad \vec{V_2} + \overleftarrow{V_2} = \vec{V_3}$$

and

$$(86) \qquad \vec{I_2} - \overleftarrow{I_2} = \vec{I_3} \quad .$$

Using (82) in (81), one gets

$$(87) \qquad \vec{V_2} - \overleftarrow{V_2} = \mathbf{z}_\ell \; \frac{z}{z} \vec{I_3} = \frac{z_\ell}{z} \vec{V_3} \quad ,$$

Add equations (85) and (87) and solve for V_2 to obtain

$$(88) \qquad \vec{V_2} = \frac{1}{2} \left(1 + \frac{z_\ell}{z}\right) \vec{V_3} \quad .$$

But,

$$(89) \qquad \vec{V_2}\Big|_{\text{at junction (2)}} = \vec{V_2}\Big|_{\text{at junction (1)}} e^{-\alpha d}$$

Thus, use equation (89) in equation (88) plus equation (84) to arrive at the resulting equation,

$$(90) \qquad \vec{V_1} = \frac{1}{4} \left(1 + \frac{z_\ell}{z}\right)\left(1 + \frac{z}{z_\ell}\right) e^{\alpha d} \; \vec{V_3} \quad .$$

The shielding effectiveness is defined by

$$(91) \qquad S.E.(db) = 20 \log \left| \frac{\vec{V_1}}{\vec{V_3}} \right| \quad .$$

During measurements with the coaxial device, comparisons of $\vec{V_1}$ and $\vec{V_3}$ are made with (1) the coaxial device in the circuit as shown in Figure 20(A), and (2) with the coaxial device out of the circuit and in its place an attenuator as shown in Figure 20(B). Thus, one has from Figure 20(B):

(92) $\vec{V_{3A}}$ = (Loss Ratio) $\vec{V_{1A}}$

also from (90),

$$(93) \quad \vec{V_3} = \frac{e^{-\alpha d}}{\frac{1}{4}(1 + \frac{z_\ell}{z})(1 + \frac{z}{z_\ell})} \vec{V_1} .$$

In the test, the attenuation is adjusted until

(94) $\quad \vec{V_{3A}} = \vec{V_3} .$

Comparing Equations (92) and (93) and using Equation (94) one gets

$$(95) \quad \text{(Loss Ratio)} \ V_{1A} = \frac{e^{-\alpha d}}{\frac{1}{4}(1 + \frac{z_\ell}{z})(1 + \frac{z}{z_\ell})} \vec{V_1} .$$

If V_{oc}, the generator voltage, is kept constant, then $\vec{V_{1A}} = \vec{V_1}$ and

$$(96) \quad \text{(Loss Ratio)} = \frac{4 \, e^{-\alpha d}}{(1 + \frac{z_\ell}{z})(1 + \frac{z}{z_\ell})}$$

Using Equations (76), (77) and (78) in (96) and using the simplification $z^2 \gg z_\ell^2$, one has

$$(97) \quad \text{(Loss Ratio)} = \frac{4 z_\ell \, e^{-\sqrt{\frac{\omega\mu\sigma}{2}} \, d}}{50}$$

Using Equation (91), one sees that the shielding effectiveness is equal to the

number of db introduced by the attenuator, or

(98)   S. E. (db) = 20 log $\dfrac{25\,e^{\sqrt{\omega\mu\sigma/2}\,d}}{2\,|Z_\ell|}$.

Now,

(99) $Z_\ell = \dfrac{\ln\frac{b}{a}}{2\pi}\cdot\sqrt{\dfrac{\omega\mu}{\sigma}} = \sqrt{\omega L_\ell R_\ell}$

and

(100) $\sqrt{\dfrac{\omega\mu\sigma}{2}}\,d = \sqrt{\dfrac{\omega L_\ell}{2R_\ell}}$,

where R_ℓ and L_ℓ are the resistance and the inductance of the lamina. Therefore,

(101)   S. E. (db) = 20 log $\dfrac{25\,e^{\sqrt{\frac{\omega L_\ell}{2R_\ell}}}}{2\sqrt{\omega L_\ell R_\ell}}$.

Expanding and simplifying, one finds that

(102)   S. E. (db) = 13.9 - 10 log R_ℓ L_ℓ -10 log f $+ 15.4\sqrt{\dfrac{L_\ell}{R_\ell}}\sqrt{f}$.

For the case of copper,

(61) L_ℓ = 10.6 x 10^{-12} henry and (61) R_ℓ = 50 x 10^{-6} ohm

and, for the case of the high-μ metal tested (assuming a μ_r of 10^4),

(103) R_ℓ = 1.33 x 10^{-3} ohm and (105) L_ℓ = 7.42 x 10^{-8} henry.

Thus, equation (102) reduces to

(104)   S. E. (db) = $166.8 - 10\log f + 7\times10^{-3}\sqrt{f}$

for the case of copper, and

(105)   S. E. (db) = 114 - 10 log f + 0.112$\sqrt{f}$,

ARMOUR RESEARCH FOUNDATION OF ILLINOIS INSTITUTE OF TECHNOLOGY

for the case of the high-μ metal tested.

Equation (104) is plotted in Fig. 14 in the same frequency range as the experimental results. As one can see from the figure, the overall behaviour of Equation (104) and the experimental results is similar, except for their widest separation by about 7 db. Equation (105) is plotted in Figure 15 for the three values of μ_r equal to 10^3, 4×10^3 and 10^4.
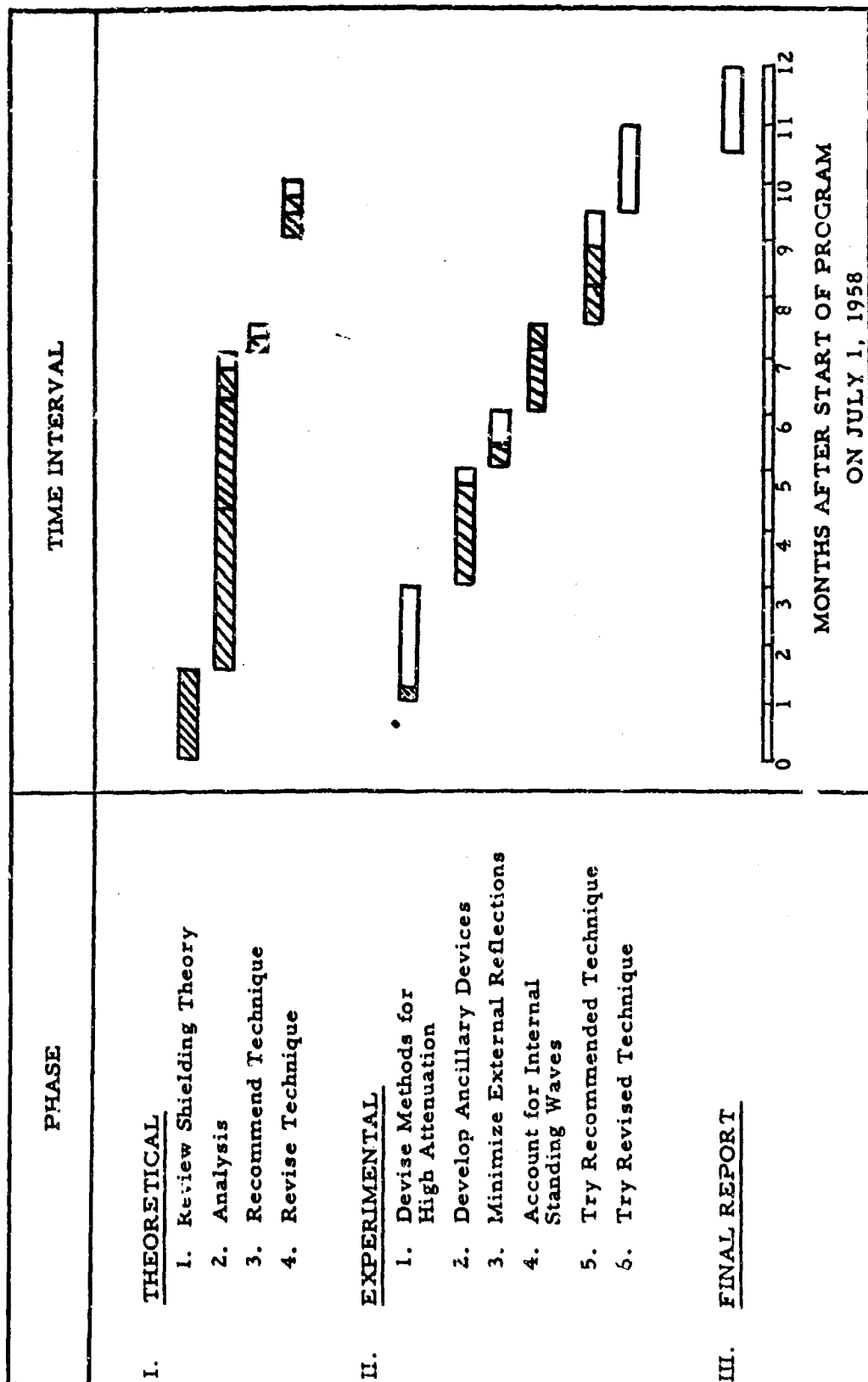
Since Equation (105) with the value of $\mu_r = 4 \times 10^3$ best fits the experimental data obtained, it is determined that $\mu_r = 4000$ over the frequency range considered, whereas the nominal value of μ_r for the material is quoted by the manufacturer to be "extremely high." It is assumed that the resistivity of the materials does not change appreciably with frequency.

5. Conclusions

Equation (102) shows the dependence of the attenuation on the frequency (for $\omega >> \frac{L_\ell}{R_{series}}$) and on the material parameters R_ℓ and L_ℓ for the case of "pure" TEM waves. However, the imperfections in the contact resistance and the magnification of the lamina dimensions mentioned previously prevent this theoretical formula from being applied directly and being compared exactly with experimental results which are obtained with the coaxial device. Moreover, this equation is not directly applicable to shielded enclosures because of size and geometry. It gives, however, an overall picture as to the effect the resistivity (implied in the shunt resistance R_ℓ of the lamina) and relative premeability (implicit in the series inductance of the lamina L_ℓ) play in introducing attenuation, as well as the dependence upon frequency.

F. Project Performance and Schedule Chart

The scheduling of the program of research is shown in Figure 21. The open areas represent planned effort while the shaded area represent completed

FIGURE 21   PROJECT SCHEDULE CHART

The chart organizes work by PHASE and TIME INTERVAL.

PHASE

I. THEORETICAL
1. Review Shielding Theory
2. Analysis
3. Recommend Technique
4. Revise Technique

II. EXPERIMENTAL
1. Devise Methods for High Attenuation
2. Develop Ancillary Devices
3. Minimize External Reflections
4. Account for Internal Standing Waves
5. Try Recommended Technique
6. Try Revised Technique

III. FINAL REPORT

TIME INTERVAL

MONTHS AFTER START OF PROGRAM ON JULY 1, 1958 — scale 0 through 12.

Legend:
COMPLETED EFFORT
PLANNED EFFORT

work. The financial status of the project is as follows:

For the period ending 31 May 1959*

Original money allocated for research	$37,672
Total expenditures	31,053
Total commitments	483
Balance available for research	6,136

It is anticipated that the expenditures for June 1959 will be approximately $3,000.

IV. CONCLUSIONS

1. The advantages of using two large loops to immerse the enclosure in a low-impedance, low-frequency field are that a pick-up loop in the center of the enclosure can then be used to provide an overall indication of performance, and a small pick-up loop probe can be employed to explore for local defects. Only one measurement is necessary at low frequencies, since the voltage induced in the pick-up loop in the absence of the enclosure can be obtained theoretically.

2. The two-loop method of measurement of shielding effectiveness at low frequencies shows that the two readings obtained by exciting the large loop outside and subsequently measuring the voltage induced in the small loop inside, or vice versa, are identical. In the analysis, the shielded enclosure is represented by a short circuited turn consisting of inductance and resistance in series.

3. The surface impedances of sheet copper (2.5 mils thick) and copper screening (22 x 22 strands per inch, 15 mils diameter) are almost

* Cost sheets for June 1959 are not available until July 20, 1959.

ARMOUR RESEARCH FOUNDATION OF ILLINOIS INSTITUTE OF TECHNOLOGY

ARF Proj. E108
Quar. Rpt. No. 4

identical at the low frequencies. Their reflection loss, which is the main loss at low frequencies, is therefore the same. The above two materials are interchangeable for shielding purposes at low frequencies. The calculated and measured shielding effectiveness to plane waves at low frequencies agree with those reported by Vasaka.

4. The presence of standing waves inside the cavity at the midfrequencies can introduce a degradation in shielding effectiveness of about 25 to 30 db (at 80 to 400 mc).

5. The coaxial testing device has been used to test shielding effectiveness to plane waves of some of the most common shielding materials such as copper, iron, aluminum, stainless steel, and high-μ metal on one hand, and copper screening on the other. Limitations of the instrument sensitivities and mechanical difficulties in reducing the lamina thickness do not allow the measurements to be taken above 8 mc at present.

6. The shielding effectiveness of copper screening to plane waves has been measured with the coaxial tester over the frequency range of dc to 400 mc. The measurements show that the shielding effectiveness to plane waves of the material decreases with frequency, being about 150 db at the very low end of the spectrum (dc to 10 kc) and about 65 db at 400 mc.

7. The coaxial testing device was used to determine the relative permeability of a high-μ shielding metal. The value of μ_r thus reported was about 4000 in the frequency range of 100 kc to 650 kc. It appears that the device is useful to determine experimentally the relative permeability of materials at radio frequencies.

V. PROGRAM FOR THE NEXT INTERVAL

The original termination of this project was 30 June 1959. However,

a time extension has been granted up to 30 September, 1959. During this last quarterly period, effort will be expended on the following aspects of the program.

1. Experimental investigation of the coaxial device for evaluating shielding materials will be continued.

2. Further investigation of the nature of generation and methods of suppression of standing waves inside shielded enclosures at the resonant frequencies will be continued.

3. Measurements at the kilomegacycle region will be concluded.

4. The final form of the test standards for measurement of shielding effectiveness of enclosures will be set up and trial test runs may be made at plants of different shielded enclosure manufacturers.

VI. LOGBOOKS

Data obtained on this project are contained in Logbooks C 8375, C 8724, C 8836, and C 8355.

<div align="right">

Respectfully submitted,

ARMOUR RESEARCH FOUNDATION
of Illinois Institute of Technology

D. P. Kanellakos
D.P. Kanellakos, Assistant Research Engineer

H. M. Sachs, Supervisor
Electronic Interference

</div>

APPROVED:

S. I. Cohn, Assistant Director
Electrical Engineering Research

ARMOUR RESEARCH FOUNDATION OF ILLINOIS INSTITUTE OF TECHNOLOGY

- 58 -   ARF Proj. 5108
                                Quar. Rpt. No. 4

ERRATA

The symbol TM_{011} appearing in the title of Figure 13, page 32 of the Third Quarterly Progress Report (Reference 2) and also on page 31 of that report should be changed to TE_{101}.